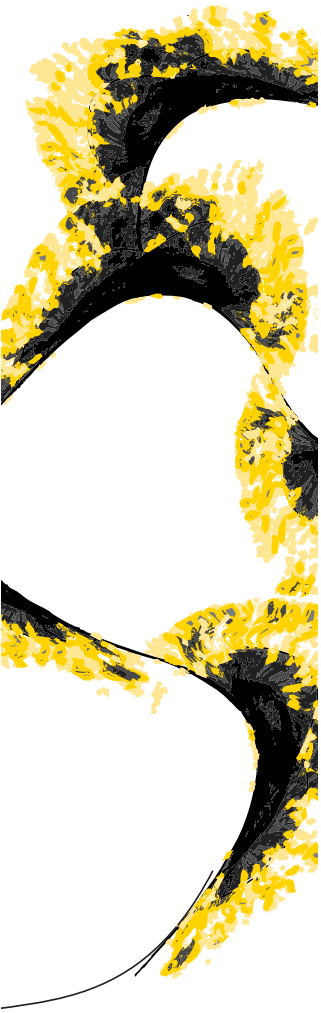

RAM ROBOTICS AND MECHATRONICS

HAPTIC FORCE FEEDBACK USING SOFT ACTUATORS IN THE CONTEXT OF ROBOTIC NEEDLE INSERTIONS

M. (Mark) Hoekstra

MSC ASSIGNMENT

Committee:
dr. ir. M. Abayazid
M.S. Selim, MSc
dr. A. Sadeghi

October, 2024

068RaM2024
Robotics and Mechatronics
EEMCS
University of Twente
P.O. Box 217
7500 AE Enschede
The Netherlands

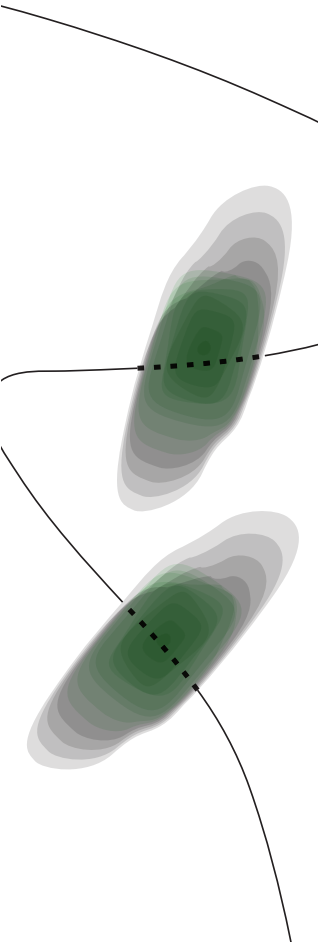

UNIVERSITY OF TWENTE. | TECHMED CENTRE UNIVERSITY OF TWENTE. | DIGITAL SOCIETY INSTITUTE

Summary

With the current trends seen in the field of surgery, MIS (minimally invasive surgery) has become increasingly prevalent due to its advantages over open surgery. These techniques also come with disadvantages, namely a limited workspace due to the small incisions, together with reduced visual and sensory information. Robotics have been introduced into this field with the aim of counteracting these difficulties. Specifically, soft robotics have shown great potential due to their compliance and controllable stiffness. This thesis aims to use pneumatic soft robotics together with a model-free control strategy to provide precise haptic force feedback, specifically in the context of needle insertions. The system in question, for this thesis, consists of two opposing soft pneumatic actuators called rPAMs. These actuators provide the main challenge for the controller due to their non-linear and hysteretic characteristics.

To achieve the goal of providing precise haptic force feedback, first, a new actuation method is proposed. This new method aims to reduce the number of control inputs from two to one. This is accomplished by coupling the pressure in both actuators, meaning only one pressure needs to be set. The position control performance was tested using both actuation methods. Showing that this change caused no significant performance loss for the position controller.

The new coupled actuation method enabled the design of a force controller that only has to give one pressure input to the system. This force controller consists of two parts, namely a feed-forward, created by performing a force characterisation on the system, and a feedback part. Initially, a PI feedback controller was tuned with 1N set-point changes. The resulting controller showed accurate force tracking performance while moving. Keeping the force error below the JND (just notable difference). Applying this controller to a realistic set-point, mimicking a needle insertion, revealed that the PI controller is too aggressive. This aggressiveness led to issues with the actuator's durability.

The durability issue led to the addition of a pressure change speed limit and a damping term in the feedback controller. The damping term was added in order to deal with the much larger overshoot introduced by the pressure speed limit. This final controller showed comparable performance to the initial PI controller, while avoiding aggressive pressure changes.

Further research was done into the degradation of the pneumatic actuators and its effect on the control parameters. This showed that the actuators do indeed change over time due to usage. Furthermore, the actuators are observed to have a 'warming up' period, in which very consistent parameter change occurred within a single measurement. However, more research is needed to gain more insight into this degradation, along with its effect on control performance.

Finally, some system redesigns are suggested. Numerous issues were encountered with the design of the force sensors and their contact point with the handle. This design issue was a big contributor to the aggressiveness of the initial controller and should be resolved before further research is conducted.

Contents

1 Introduction

1.1 Robotics in Surgery

An important development that is currently being made in the field of surgery is moving from open surgeries (invasive surgeries) to minimally invasive surgeries (MIS) or noninvasive procedures whenever possible. These three types of medical intervention differ in their degree of 'invading' the body by way of incisions. Open surgeries make use of larger incisions in order to gain access to the parts of the body that need to be operated. MIS uses much smaller incisions through which tools and a camera are inserted to perform the surgery. A common example of this is laparoscopy which is a medical intervention used for surgeries and examinations in the stomach and pelvis areas. Noninvasive procedures do not breach the body in any way. Examples would be procedures using x-ray, MRI or CT imaging technologies.

MIS has many clear advantages over open surgeries, predominantly less trauma on the body, other benefits include: reduced pain, less blood loss, minor scarring and shorter recovery times for patients. However, MIS also brings some significant difficulties with them. Due to the nature of MIS procedures, they are much more challenging to perform. Surgeons have to have specific training in order to know how to navigate a highly limited workspace with significantly reduced visual and sensory information. Despite all these extra difficulties, however, MIS is still being implemented progressively more. A large contributing factor to this transition is the investing in research and technology development in the field of surgical medicine to improve the aforementioned difficulties (Hamed et al., 2012; Hatzipanayioti et al., 2021).

Concepts of MIS can be traced back to the end of the 19th century. The first laparoscopic procedure performed on a human dates back to 1910 performed by H.C. Jacobaeus. The first patients receiving this treatment all suffered from ascites. These operations were easy and problem free. The treatment on patients without ascites was considerably more perilous. Due to the risk of intestinal injuries being substantially higher. Jacobaeus concluded from this that laparoscopy was not fit to be used in non-ascites patients due to the increased risk of the patients health (Hatzinger et al., 2006).

These early forms of MIS have turned into a realistic alternative procedure for specific surgical interventions. Mainly due to more recent technological developments like enhanced high resolution video imaging and improved instrumentation. The actual reality of this paradigm shift, however, is that it predominantly only saw success in high volume procedures with low complexity. High volume meaning they are performed mass amounts per year, which means there are a myriad of opportunities to implement, experiment and perfect MIS procedures (Mack, 2001).

The current movement in surgical medicine is leaning towards the field of robotics. Due to the technological advancements that can facilitate the reduction of invasiveness in more complicated procedures. Initially, this research primarily focused on providing surgical medicine remotely which is also known as telesurgery. Subsequently, increasing research is being done to bring robotics into the field of MIS as well. The areas of research for MIS predominantly include navigation and guidance, dexterity enhancement, and virtual reality (VR). Dexterity enhancement shows especially promising advantages, which includes movements with supernatural precision and enhanced force feedback for the surgeon. These features will allow surgeons to perform tasks at new levels of precision. This would make the previously impossible procedures possible (Mack, 2001).

The improvement of force feedback will presumably play a significant role in the movement towards MIS. Force feedback will not only enable supernatural precision procedures and telesurgery. It will additionally be a major component for creating realistic feeling VR environ-

ments (Hamed et al., 2012). These VR environments are excellent training tools for surgeons to perfect MIS techniques. Furthermore, force feedback improves surgery quality by reducing the amount of force applied to tissues during operation (Wagner, Stylopoulos and Howe, 2002). Leading to less trauma on the patients body and faster postoperative recovery times.

Soft robotics shows great potential for the difficulties faced in MIS. Soft robotic actuators are compliant, have a controllable stiffness and are ideal for interacting with humans (Runciman, Darzi and Mylonas, 2019; Skorina, Luo, Oo et al., 2018). These qualities make soft actuators prime candidates for providing haptic force feedback. The specific actuator used in this research is known as the rPAM (reverse pneumatic artificial muscle). It is a hollow silicon tube. When pressurised it elongates, which is how it provides its actuation. These actuators are simple and inexpensive to produce. They have an excellent force to weight ratio, and additionally are MRI and CT compatible.

The specific focus of the thesis is for providing haptic force feedback in the context of needle insertion procedures for biopsies and ablations. This context comes with certain limitations and requirements that must be met. First of all the system is relatively slow moving (insertion speeds between 2.5 - 5 mm/s). Second, typical forces seen in these type of procedures go up to 1.7N for human liver tissue (De Jong et al., 2017) and approximately 3N for bovine liver tissue (Okamura, Simone and O'Leary, 2004). The system will need to be capable of producing these forces at minimum. Force production beyond these numbers can be beneficial for providing enhanced haptic force feedback, however, is not a requirement.

1.2 Thesis Objective

The growing interest in MIS and telesurgery has caused increasing research into providing control using soft robotics. Currently, soft pneumatic actuators have shown great performance for general position control. More precise control tasks, for instance providing haptic force feedback, is seen as problematic for these types of actuators. This thesis aims to show the potential of providing precise force control with soft pneumatic actuation coupled with the difficulties accompanied with this task.

The research in this thesis is a continuation of two previous theses, which mainly focused on creating a physical test setup together with initial control efforts. This physical setup includes two soft pneumatic actuators, which will be responsible for providing actuation and force feedback. The main difficulty lies in the characteristics of these actuators. They show non-linear and hysteretic behaviour. The research questions to be answered are as follows.

- Can a model-free controller deliver precise force feedback while dealing with the non-linearity and hysteretic behaviour of the soft pneumatic actuators?
  - Can the actuation method be simplified for force control and does this impact the performance of the position control?
  - Is the controller able to keep the error below the just noticeable difference (JND)?
  - How does the durability and deterioration of the actuators affect the force and position control performance?

The thesis starts with a literature review. In here the current state of the art is reviewed with additional research and background information necessary for the research in this thesis. Following is a description of the results of the previous two theses with a description of the physical test setup. From there on the research of this thesis is documented in which the above research questions will be answered.

2 Background

This chapter starts off with a literature review (Section 2.1) showcasing research relevant to this thesis. This is followed by background information about the current system (Section 2.2). This section is a summary of the previous work done on the system. Giving the reader the relevant information needed in the thesis.

2.1 Literature Review

2.1.1 Soft Actuators and rPAMs

Soft actuators have gained an increased amount of interest over the years due to their considerable potential. They show clear benefits over rigid actuators when the system needs to deform and interact with its environment. There are many different types of soft actuators, however, this thesis focuses specifically on the rPAM (reverse pneumatic artificial muscle). This actuator is a slightly modified version of the PAM which was first introduced as the McKibben muscle by Klute, Czerniecki and Hannaford (1999). The PAM actuator is a tube like structure made of soft materials wrapped in a braided mesh. When pressurized, this tube will expand and grow radially, which will contract the muscle due to the mesh that is wrapped around it. The rPAM is very similar, however, the braided mesh is modified. Meaning instead it constraints the radial expansion of the tube. This will cause the tube to extend instead which results in the reverse actuation compared to the PAM.

El-Atab et al. (2020) groups review shows that the main use for pneumatic soft actuation is simple tasks. Namely tasks that do not require high amounts of precision. The reason for this is that these actuators are very difficult to model due to their non-linearity and hysteritic behaviour. This makes using them for precision control tasks more difficult despite their clear benefits over their rigid counterparts.

These pneumatic soft actuators are becoming increasingly popular. Increasing the amount of research into their controllability. Skorina, Luo, Oo et al. (2018) made an analytical and a finite elements approximation model of an antagonistic rPAM actuated revolutional joint. Their analytical model consists of two components namely, the constraint model and the material model. The constraint model takes into account the geometries and their constraints needed for the desired expansion. The material model uses the Ogden model taking into account the material properties used in the actuator. The results of these modeling efforts can be seen in Figure 2.1.

As can be seen in the modeling results of Skorina, Luo, Oo et al. the predictions are close, however, certain pressure and load combinations can still cause very clear errors in the model.

2.1.2 Antagonistic Actuation

Robotic systems frequently see the use of antagonistic actuation setups. This work is focused on using soft actuators for force and position control. Meaning it will be limited to this area of antagonistic actuation as well. Antagonistic actuation is by a large part inspired by how the human muscles function. Therefore, it is used a lot for the design of rehabilitation devices (e.g. Chi et al., 2021). Additionally, these systems often use soft actuators since they need to interact with patients.

There are multiple different benefits to using actuators antagonistically. The most obvious one is that it allows for actuation in both directions. Furthermore, by using soft actuators the stiffness felt at the end effector can be controlled. This enables the ability to perform realistic haptic feedback (Medrano-Cerda, Bowler and Caldwell, 1995).

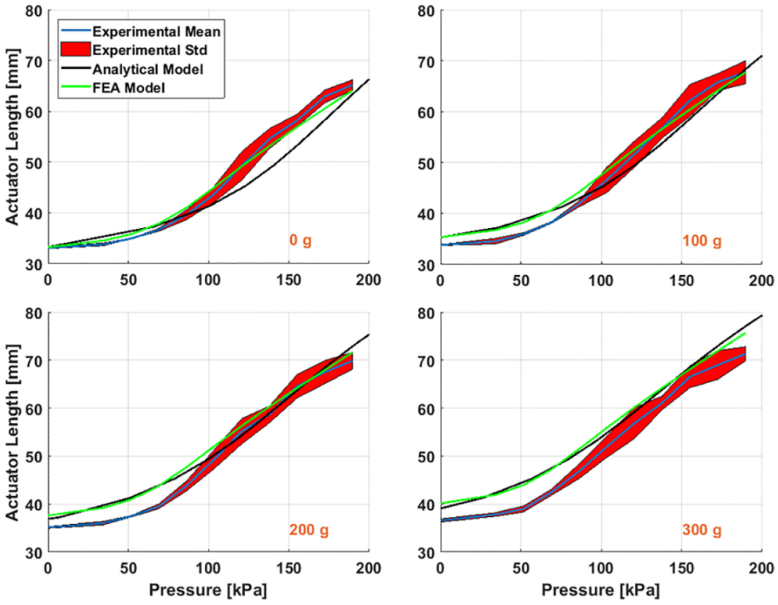

Figure 2.1: Angle prediction results of using the analytical model and the finite elements approximation (Skorina, Luo, Oo et al., 2018)

A potential downside to using an antagonistic setup is that it needs multiple control inputs. The most commonly used method to handle this problem is to make one input depend on the other. This means that the two actuators are always in opposition to each other (Skorina, Luo, Ozel et al., 2015).

Andrikopoulos, Nikolakopoulos and Manesis (2014) developed a control strategy for both a single and antagonistic PMA (pneumatic muscle actuator) setup. The antagonistic scheme they used initially set a maximum pressure value. The pressure that was given by their controller was then given to one of the two actuators. The pressure of the second actuator was then calculated by taking the max pressure and subtracting the pressure of the first actuator.

$$P_2 = G - P_1 \tag{2.1}$$

With:

- G: Max pressure
- P_1: Pressure in actuator 1
- P_2: Pressure in actuator 2

Equation 2.1 is a simplified version of what was used. Andrikopoulos, Nikolakopoulos and Manesis added extra safety by making sure P_2 cannot become negative.

Ning et al. (2019) used a control strategy for a source-replica antagonistic joint by using both PAMs and water hydraulic muscles. They used a slightly different antagonistic scheme. Instead of setting a maximum pressure they defined an average pressure. The controller then outputs a ΔP which is added or subtracted from the average pressure.

$$P_1 = P_{avg} + \Delta P \tag{2.2}$$

$$P_2 = P_{avg} - \Delta P \tag{2.3}$$

With:

- P_{avg}: Average pressure defined before

- ΔP: The pressure change from the controller output

2.1.3 Haptic Feedback in Medical Applications

A lot of haptic feedback devices already exist and have been successful. However, as mentioned in the introduction this research is in the context of needle insertion procedures. This gives some limitations in the devices that are considered. Selim, Dresscher and Abayazid (2024) review shows numerous haptic devices, specifically in the aforementioned context.

The first notable haptic device mentioned, is the one developed by Maurin et al. (2004). They developed a tele-operated haptic feedback system that is able to perform needle insertions in a CT scan environment. It is, however, not designed to be operable in an MRI environment. MRI poses some extra design requirements since it is not possible to use any ferro-magnetic materials.

Studies on developing devices that are operable in MRI have also been carried out and reviewed in Selim, Dresscher and Abayazid (2024). These studies all use different MRI compatible systems. Tse et al. (2012) used ceramic piezo-electric actuators. Shang et al. (2013) used pneumatic actuators together with a load cell and fibre optic force sensors for the haptic feedback. Mendoza and Whitney (2019) used hydrostatic actuators instead making force measurement estimations based on the hydrostatic pressure measurements. These MRI compatible needle insertion devices all showed promising results. However, still more research and work is needed before these systems can be applied in real situations.

2.1.4 Model-free Control Strategies

Model-free control strategies do not need a precise model of the system to be controlled. These strategies are widely used for tracking and disturbance cancellation. Specifically in systems that show non-linear and hysteretic behaviour, since these systems can be very complex to model accurately (Medrano-Cerda, Bowler and Caldwell, 1995).

These model-free control strategies have been used before on actuators similar to rPAMs. Recent studies have researched the use of an advanced non-linear PID control structure (AN-PID) (Andrikopoulos, Nikolakopoulos and Manesis, 2014). In the AN-PID structure the error terms are separately adjustable for each of the three PID parts. This gives more controllability in these specific terms.

Another adjustment made to the standard PID algorithm is the subdivision of the workspace. The controller parameters have been tuned specifically for each subsection. The linearisation inside each of the subsections helps deal with non-linearity in systems. A potential problem with this division of the workspace occurs when parameters vary significantly between subsections. Switching between these subsections can cause abrupt changes in control parameters and signals. To prevent this potential issue, a bumpless transition mechanism was made which smoothly transitions between the different subsections of the workspace.

2.1.5 Realistic Needle Insertions

The scope of this thesis, as mentioned before, is limited to needle insertions. Understanding the behaviour and situations the controller will be subjected to is important for the design and tuning of said controller. Motheram (2023) have done extensive research into the axial force experienced while performing needle insertions into bovine livers. Figure 2.2 shows one of the force profiles that was measured.

To model this the force profile was separated into three distinct terms. The insertion starts with puncturing whatever tissue the needle needs to be inserted into. The initial tissue puncture is indicated in Figure 2.2. It consists of an exponentially rising force followed by a sudden drop

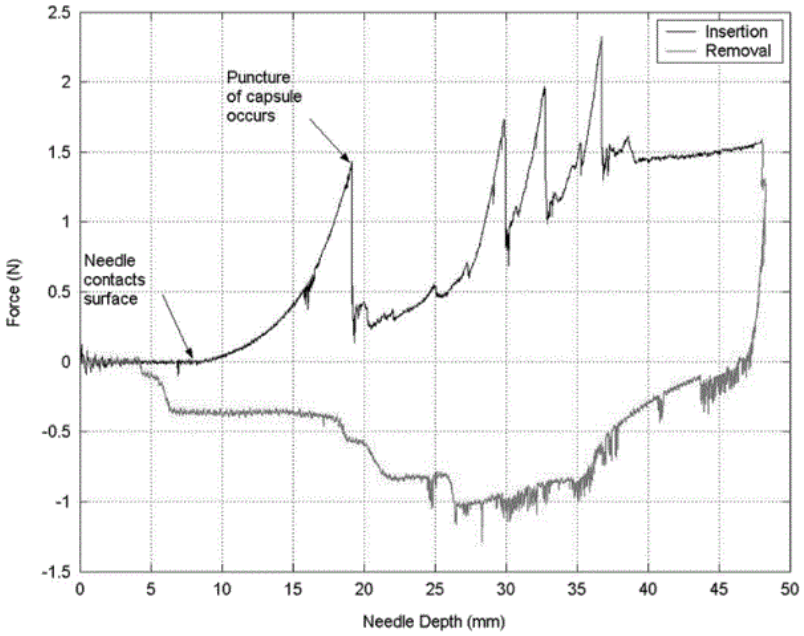

Figure 2.2: Axial force measurement during insertion and removal of a needle into a bovine liver. (Okamura, Simone and O'Leary, 2004)

denoting the puncture of the tissue. Okamura, Simone and O'Leary decided to model this rise in force using the quadratic function seen below in equation 2.4.

$$f_{puncture}(z) = a_1 z + a_2 z^2 \tag{2.4}$$

With:

- $f_{puncture}$: puncture force [N]
- z: needle position [mm]
- a_1, a_2: constant coefficients

After this first puncture, the main contributors to the force acting on the needle are the cutting and friction force. The cutting force is relatively constant throughout the insertion assuming the tissue is uniform. The friction force, however, slowly increases linearly with insertion depth. The deeper the insertion the more surface area of the needle is in contact with the tissue. Figure 2.3 below shows these two forces separately.

2.1.6 Human Force Perception

The function of the system being researched in this thesis is to provide haptic force feedback to a human user. The required precision of this force feedback depends on how sensitive a human user is to force variations. To gain insight into this sensitivity the JND (just noticeable difference) is used. The JND indicates the minimal force variation perceivable by humans. JND can be indicated simply as a force or as a percentage of the reference force. The JND is dependent on numerous conditions namely: what part of the human body is experiencing the force and what the absolute value of the forces being encountered is. Two situations that are relative to this thesis are the human finger and the combination of the human hand with arm.

For the finger, Shimoga (1993) states it is capable of sensing force variations of 0.5N. Tavakoli, PateI and Moallem (2004) use the same JND as Shimoga, however, adding to the statement saying the human finger is able to sense force variations of ±7%. The direction of the forces being applied is not mentioned.

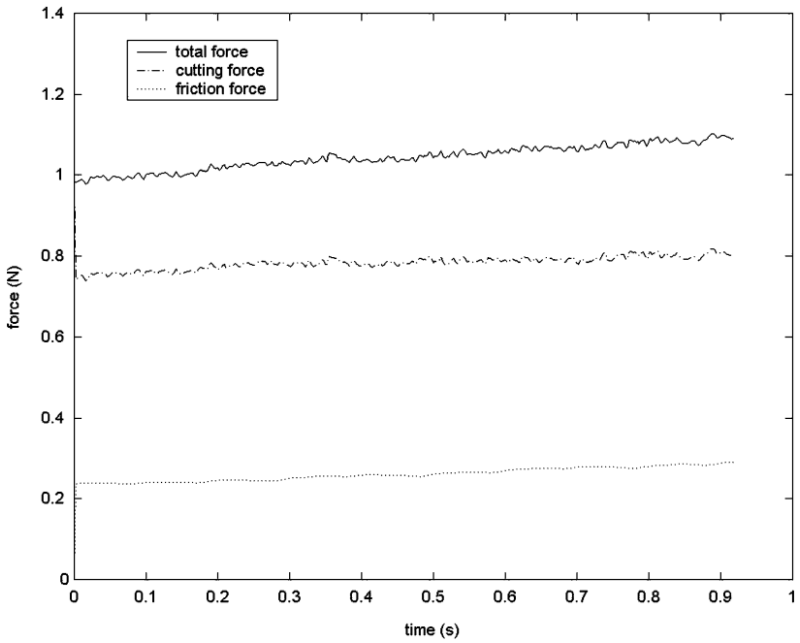

Figure 2.3: Forces on the needle tip during insertion at 3 mm/s. The total force is separated into its cutting force and friction force components. (Okamura, Simone and O'Leary, 2004)

Reference [N]	JND [%]	JND [N]
-5.99	15.3	0.916
-3.28	16.3	0.535
-1.80	18.0	0.324
-0.87	18.1	0.157
-0.54	25.7	0.139
0.50	31.6	0.158
0.83	22.7	0.188
1.79	15.7	0.281
3.26	17.0	0.555
5.98	9.6	0.574

Table 2.1: Table showing the parallel force sensitivity of the human hand-arm system expressed in JND for different reference forces.

The sensitivity of the human hand with arm to force variations has been researched more in-depth by Vicentini et al. (2010). The JND results of parallel forces to the hand with arm can be seen in Table 2.1 below.

2.2 Current State of the System

The research in this thesis will build upon the work done by three previous students. The student who started this project is A.L. Verhoef. She was a biomedical technology bachelor student who dedicated her BSc thesis to creating the first iterations of the haptic feedback device. This work was then further improved and built upon by two Master students. M. Motheram's research was devoted to designing and developing a 1-DOF (degree of freedom) needle insertion robot with integrated force sensing (Motheram (2023)). This device is controlled by the previously mentioned pneumatically driven haptic feedback device. E.S. Gudmunsson worked in parallel with Motheram and focused on improving Verhoef's initial design (Gudmundsson, 2023). The addition of extra force sensors and enhanced friction characteristics were the primary improvements. This improved the system's overall controllability. Addition-

ally, Gudmundsson made some initial control efforts along with user trials testing the haptic feedback capabilities.

The overall project has already seen a considerable amount of research and work. Next, the current physical setup is described in order to get the reader up to speed. This is followed by a summary of the model and control efforts performed by Gudmundsson.

2.2.1 Physical Setup

The current setup consists of the pneumatically driven haptic feedback device (source device), which controls the movement of the 1-DOF needle insertion robot (replica device). The description of the needle insertion device, designed by Motheram, is left out since this thesis solely focuses on the haptic feedback device.

The source device consists of a main block to which all the sensors and actuators are connected. This block is indicated in Figure 2.4. The handle is connected inside this block and has a very minor freedom of movement to the left and right. This movement allows the handle to make contact with one of the force sensors inside the block. These force sensors are responsible for measuring the force produced and felt by the user.

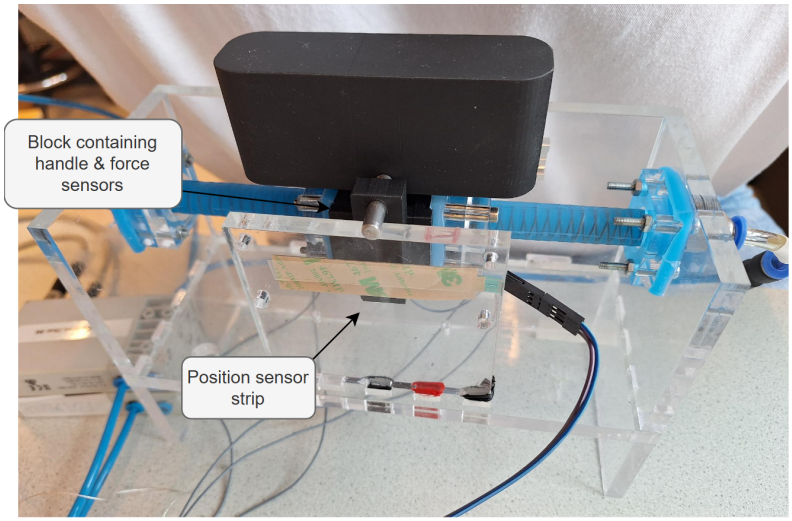

Figure 2.4: Side view of the pneumatic haptic feedback device.

Additionally, a potentiometer strip is connected as shown in the same figure. This strip acts as the position sensor for the handle-block. There is a small contact point between the strip and the device. This contact point slides across the strip as the handle-block is moved.

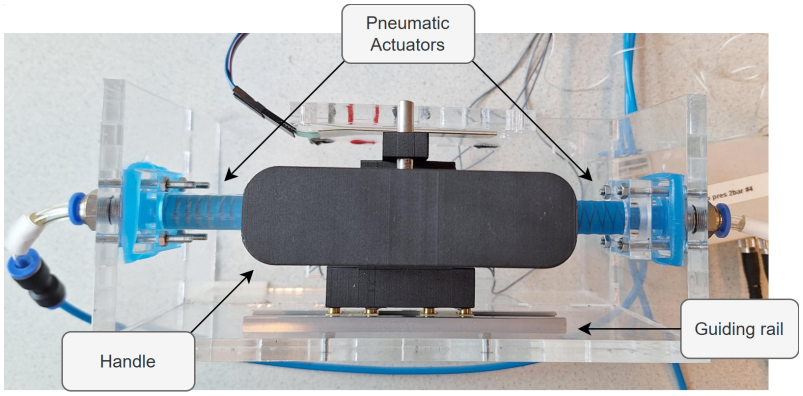

Figure 2.5: Top view of the pneumatic haptic feedback device.

Two opposing sides of the main block have pneumatic rPAM actuators connected to them, which are indicated in Figure 2.5. This figure also shows the guiding rail along which the block can move.

2.2.2 Soft Actuators

The soft actuators used in this setup are known as rPAMs and have the characteristic of elongating when pressurised. These actuators are made using a rubber silicone (Ecoflex 00-50), moulds and fishing line. There are two moulds used to create the actuators. The first mould (Figure 2.6) will create the inside part of the actuator.

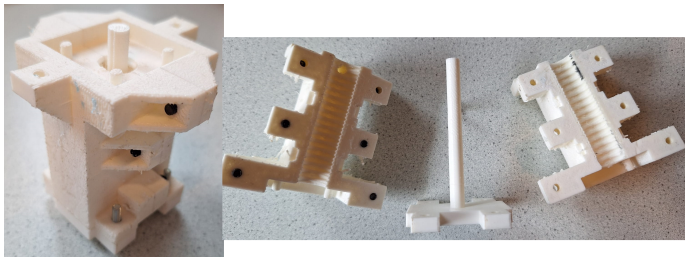

Figure 2.6: First mould put together and apart. Clearly showing the grooves in the right picture.

The final product of this mould has small grooves on the outside of the long cylinder section. These grooves serve as a guide for the fishing line. The fishing line is wrapped around the actuators and serves as the previously mentioned braided mesh. This restricts the expansion of the actuator to allow elongation only. The right picture in Figure 2.7 shows the inner actuator wrapped in the fishing line.

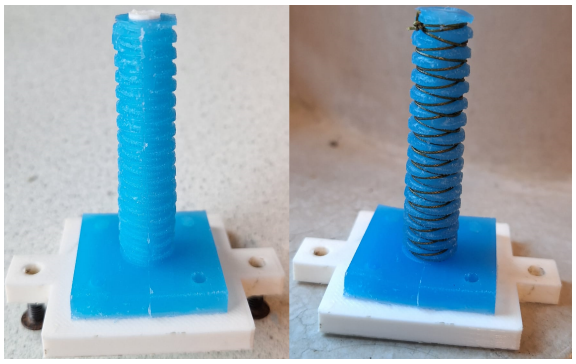

Figure 2.7: Inner part of the actuator on the mount used in the moulds. Clearly showing the grooves in the actuator. The actuator on the right is wrapped in the fishing line.

After the fishing line is wrapped around the cylinder it will go into the second mould. This mould is responsible for the outside part of the actuator. The second mould completely encases the fishing line in silicone. This second mould, along with the final resulting actuator, can be seen in Figure 2.8.

2.2.3 Control Efforts

The control efforts made by Gudmundsson consist of a feed-forward position controller and a PID feedback force controller. The feed-forward controller maps the input pressure range to the resulting position. This mapping can be seen in Figure 2.9.

Figure 2.9 (left) clearly shows the non-linear behaviour of the pneumatic actuators. Gudmundsson resolved this by adding a minimum (static) pressure. This largely linearised the mapping, allowing for a relatively simple mapping of the pressure to position. The resulting pressure versus position plot can be seen in Figure 2.9 (right).

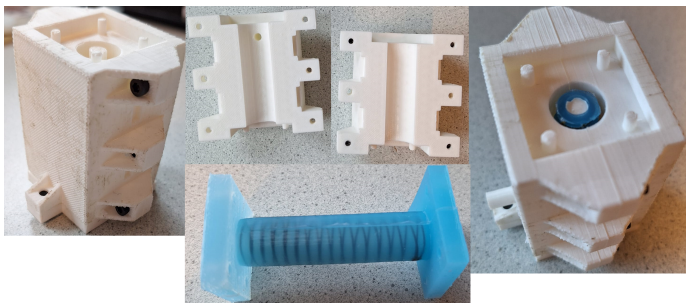

Figure 2.8: Second mould put together and apart. Along with the final resulting actuator.

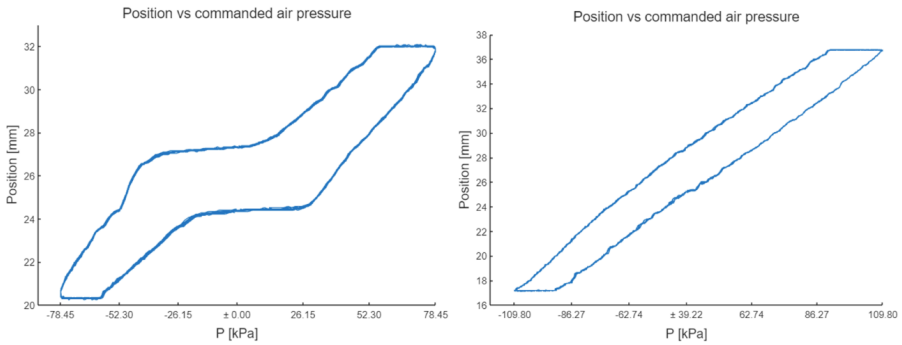

Figure 2.9: Pressure versus position mapping plot. (Left) Before linearisation with static pressure. (Right) After linearisation with static pressure. Plots made by Gudmundsson (2023)

Even though this minimum pressure did linearise the system to a large extent, the system still suffers from hysteresis. This is handled by making two linear fits of the pressure versus position mapping. Each fit corresponds to a direction of movement. The feed-forward controller will simply switch back and forth between the two fits depending on which direction the user is moving the handle. This position controller showed excellent performance and ability to keep the handle in its current position after releasing. Additionally, it greatly reduced the force required to move the handle through the workspace.

As aforementioned, a PID controller is responsible for the force control on the handle. This controller adds its output to the value of the position controller. Additionally, the force control is done only with one of the two actuators. The controller parameters are manually tuned with a sinusoidal set-point. The resulting tracking performance can be seen in Figure 2.10.

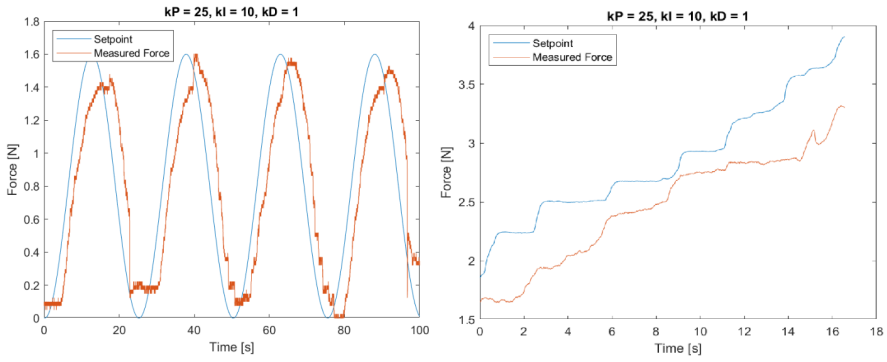

Figure 2.10: Resulting tracking behaviour with manual tuning on sinusoidal set-point input (left). Force tracking performance with ramp set-point (right). Plots made by Gudmundsson (2023)

3 Materials and Methods

This chapter is dedicated to explaining the methods used for the control efforts along with the reasoning behind them. First, a change in actuation method will be proposed (Section 3.1). This is followed by how the proposed method will be compared to the old method. This section ends with a short description of changes made to the physical system and the position control model made by Gudmundsson.

Section 3.2 is dedicated to describing and explaining the force controller being proposed in this thesis. This section is split up in two parts. The first part describes how a force characterisation of the system is made, which is used as a feed-forward controller. This is followed by the second part, which explains the different terms of the feedback controller.

The next section (Section 3.3) combines the two parts of Section 3.2 and shows how it is realised in a Simulink model. This section ends with a description of how all the control parameters will be tuned for the needle insertion scenario.

Section 3.4 is the final section and describes the methods used to gain more insight into the degradation of the actuators.

3.1 Actuation

As mentioned before, this section describes the changes proposed to the actuation method of the haptic feedback system. Additionally, the reasoning behind these modifications will be explained. The old actuation method only actively uses one of the two actuators at a time. This in itself is not a cause for concern and showed the ability to perform high accuracy position control. However, providing haptic force feedback proved more challenging. This ended in the decision to only use one of the two actuators for providing force feedback. This section proposes a method of actuation which simplifies providing force control and enables the use of both actuators.

The main complication for the force control is that both actuators are completely separate, which makes the system a two input system. As shown in the literature review (Section 2.1.2), coupling the pressure in both actuators is a commonly seen simplification. This means that the system is simplified to a SISO (single input single output) system. This coupling will be done in a similar way as described in the literature review. One of the actuators will be allowed to take any pressure inside a specific pressure range. This pressure will then be subtracted from the maximum pressure to find the pressure in the opposing actuator. Equation 3.1 shows this relation more clearly.

$$P_{a2} = P_{max} - P_{a1} \tag{3.1}$$

With:

- P_{a1}: Pressure in actuator 1 [bar]
- P_{a2}: Pressure in actuator 2 [bar]
- P_{max}: Maximum pressure in pressure range [bar]

The old actuation method uses a pressure range from 0.39 to 0.94 bars. The minimum static pressure of 0.39 bars linearises the system substantially. Pressures below this minimum do not generate enough force needed to move the handle-block. Having this minimum pressure is not strictly necessary for the new method. The proposed actuation will always have at least one actuator above the minimum pressure. This means that the actuators will be able to move the handle-block at any given pressure combination. Adding these lower pressures to the pressure

range introduces non-linearity in the position-pressure plot. Due to this, the minimum pressure of the coupled actuation is also set at 0.39 bars. Equation 3.2 shows the relation between the pressures in both actuators.

$$P_{a2} = P_{max} - P_{a1} + P_{min} \tag{3.2}$$

With:

- P_{min}: Minimum pressure in pressure range [bar]

The maximum pressure will enforce operation within a safe pressure range. Safe here meaning, that the actuators are not breaking due to too high pressures and the actuators do not buckle. Buckling here refers to when the actuators change their shape and start bending. This unwanted behaviour can be seen in Figure 3.1. This results in very non-linear behaviour and therefore should be avoided. The actuators made during this project had a slightly higher stiffness than the ones made by Gudmundsson. This led to a smaller workspace for the movement of the handle. The maximum pressure was slightly increased, since the higher stiffness also made the actuators more resilient to buckling. The new maximum pressure has been set at 1.02 bars.

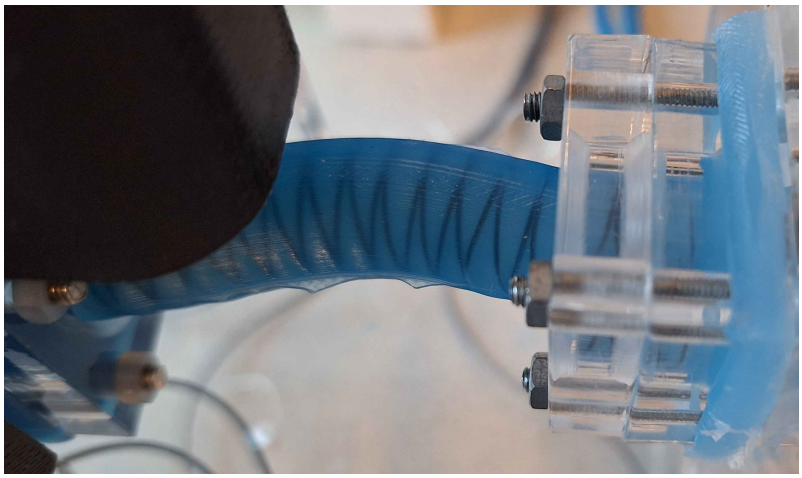

Figure 3.1: Image showcasing actuator buckling.

The proposed coupled actuation method simplifies the controller inputs for force control. However, this change in actuation should not negatively impact the position control performance. Therefore, the position controller will be tuned for both the actuation methods in order to compare their performance. The tuning method for the uncoupled actuation method is exactly the same as described by Gudmundsson. For the coupled actuation, the same steps were taken as for the uncoupled. However, adjustments in the code and models were made to account for the different actuation method. The first step is to input a sinusoidal pressure into the system that spans the entire pressure range. These different inputs can be seen in Figure 3.2. This figure also gives a clear visualisation of the two different actuation methods.

A notable difference between the methods in Figure 3.2 can be seen in the overall pressure in the system. In the uncoupled method, the overall pressure will peak when one of the actuators is at the maximum pressure. In the coupled method, however, this peak overall pressure is maintained throughout the entire pressure range. The difference in these overall pressure profiles could allow for faster buckling with the coupled method. This would mean the workspace using this method would have to be reduced. This sacrifice is deemed worth making if it results in a much simplified force controller. Additionally, this sacrifice in workspace can be 'won back' by other means (e.g. changing the actuator dimensions).

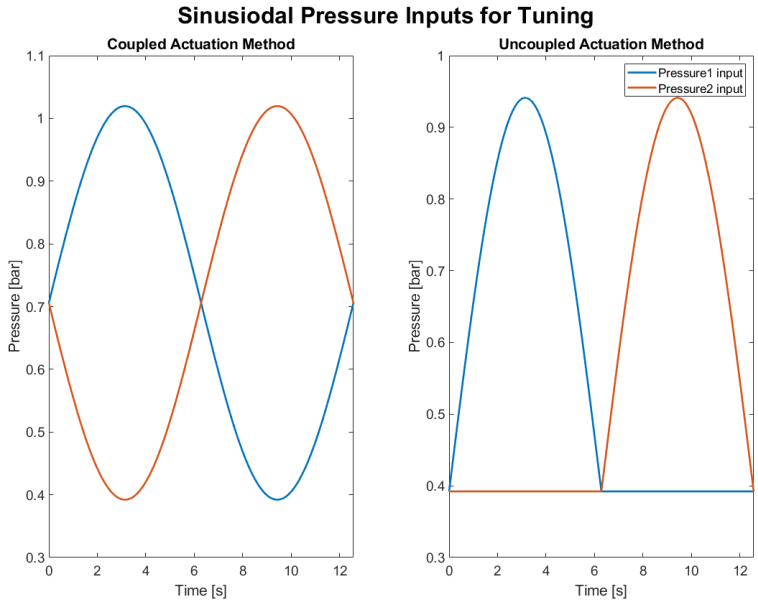

Figure 3.2: Showing the coupled and uncoupled sinusoidal pressure inputs used for the feed-forward position control tuning.

The next steps are the same as described by Gudmundsson. Two linear fits are made on the indicated sides, shown in Figure 3.3. Each side's linear fit corresponds to one of the directions of movement.

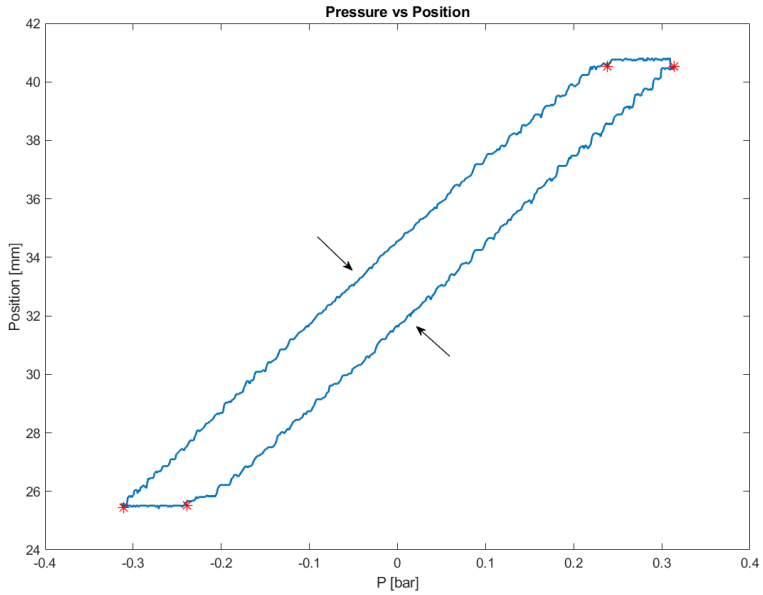

Figure 3.3: Pressure vs position plot indicating both sides used for the linear fits. The pressure values on the x-axis are left over from Gudmundsson's code and do not directly make sense for the new coupled method. This has no effect on the final linear fit.

These linear fits are made for both actuation methods and used in the position control model originally designed by Gudmundsson. This model included logic, determining which actuator to use. This has been removed for the coupled actuation method since its not needed. For

the coupled method instead, the pressure of one of the actuators is calculated using the feed-forward controller. The second actuator's pressure follows from Equation 3.2.

3.1.1 Minor System and Model Changes

The Simulink position controller model is largely the same as used by Gudmundsson. Apart from a change made to the switching between the two linear fits, described above in Section 3.1. Originally, the model checked which force sensor was reading a value above zero. Later, it was discovered that the force sensors will always be above zero even though the handle is not in contact with the sensor. This nonzero force read-out was taken into account for the switching between movement directions.

Additionally, the handle had too much freedom of movement inside the handle-block. This caused the contacting point between the force sensor and the handle to be inconsistent. Consequently, leading to wildly inconsistent force measurements. Custom made bushings were 3D printed out of Nanovia PC-PTFE. This created a significantly more consistent force read-out, however, it also increased the internal friction between the handle and the bolts. Lubrication was added to decrease this friction.

The friction inside the guiding rail was also too high. This led to stuttery movement of the entire system. The same lubricant was used to decrease this friction as much as possible.

3.1.2 Comparison with Previous Actuation Method

As aforementioned, the position controller will be tuned using both actuation methods in order to compare their performance. Two comparison experiments will be carried out. First, the backlash of the handle after release will be tested. Second, the force reduction, while moving the handle through the workspace, is compared. The last measurement is not completely relevant to the desired final system, since the position controller would ideally solely be used when the handle is not moving. It was, however, a relevant part for the final system designed by Gudmundsson. This is why it is still seen as a relevant comparison between the two actuation methods, which can provide insight in the differences in behaviour.

3.2 Haptic Force Control

The following section is dedicated to the design and modeling of the force controller. In the previous design made by Gudmundsson, the force and position controllers worked together. In contrast to this, the new design assumes complete separation between these two controllers. The force controller is discussed here on its own. The total force controller will consist of a feed-forward and a feedback part. First, in Section 3.2.1, the feed-forward part is discussed, which is created by performing a characterisation of the system's force response. Subsequently, an explanation of the different feedback terms is given in Section 3.2.3.

3.2.1 System Characterisation

The goal of this part of the controller is to create some form of mapping using measurements performed on the system. This will create a characterisation of the system's force capabilities, providing a first estimate of force control. The system can be thought of as a mass with springs and dampers connected on each side. These springs and dampers represent the pneumatic actuators. A free body diagram of this system can be seen in Figure 3.4.

At a first glance, Figure 3.4 seems like a straightforward system. The complexity comes from both the stiffness and damping coefficients. These coefficients are dependent on pressure and position. This means that the force produced by the actuators is dependent on two variables, which drastically increases the number of measurements needed to carry out the characterisation. There are two options to simplify and reduce the number of required measurements.

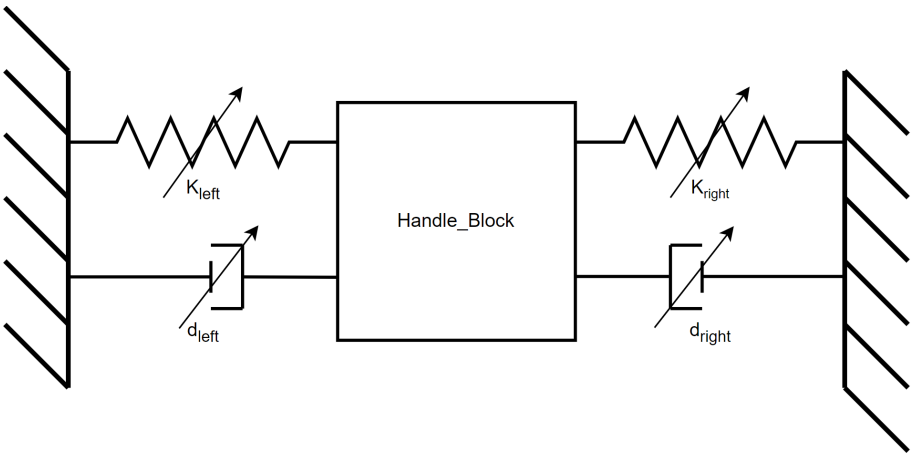

Figure 3.4: Free body diagram representation of the haptic force feedback device.

The first option is to discretise the position workspace. The force capabilities can then be measured at each discrete position by cycling the pressure through its range. This method has the benefit that no human interaction with the system is necessary, which will remove human error from the characterisation. The downside for this method, however, lies in the design of the system itself. The actuators are able to produce a force on the handle-block from both sides. These forces are measured by force sensors within the handle-block. However, the handle only makes contact with one of the sensors at a time. To switch to the other sensor, the handle will slide within the handle-block until in contact with the second sensor. This is problematic for the force measurements. Locking the handle in a specific position will change the pressure range that produces a force on one of the sensors. The handle switching from one sensor to the other is very unpredictable and should not be included in the force measurement. Therefore, this method is not viable.

In the second method the pressure range will be discretised instead. The force will then be measured at each discrete pressure while the handle is moved through the workspace. This method does have the drawback of human interaction. To combat this, the measurements will be repeated multiple times to reduce its effect.

The first step to perform this method of characterisation is discretising the total pressure range. The pressure range used in Section 3.1 is 0.39 to 1.02 bars. This minimum pressure, however, is not needed anymore, since the goal here is providing force and not movement. Therefore, the lower pressures are also included in the range for force control. The total pressure range then becomes 0 to 1.02 bars. This pressure range is discretised into fourteen different pressures. This number was chosen due to the type of input given to the pressure regulators. The regulators take a number between 0 and 255 corresponding to 0 and 2 bars, respectively. This means that the pressure range for force control goes from 0 to 130, hence the fourteen different pressures corresponding to steps of ten. Figure 3.5 shows a clear visual representation of the pressure range and its discretisation.

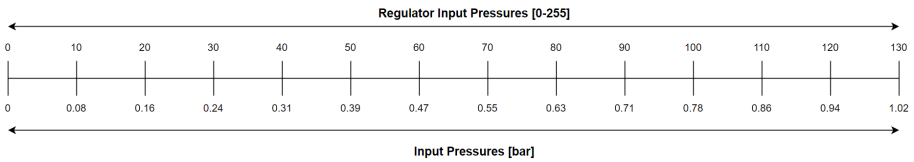

Figure 3.5: Pressure range and discretisation shown in bars and pressure regulator inputs. This pressure is for only one actuator. The pressure for the second actuator follows from Equation 3.2

The next step is performing force measurements for each discretised pressure. This is done by pressurising the actuators at one of the aforementioned pressures. Then moving the handle slowly at constant velocity, pushing against one of the actuators. The measurements have to be performed at constant velocity, since accelerating the mass will add an extra force. This force is not produced by the actuators and should therefore be minimized.

These measurements are repeated for each discrete pressure combination. To prevent buckling, two pressure combinations have been excluded. These pressure combinations moved the handle-block the furthest into the pushing direction before any force was applied. The actuator then very quickly starts buckling when applying a force on the handle with these pressure combinations, essentially getting squished.

As mentioned before, these measurements require human interaction with the system, which makes these characterisation measurements error prone. To reduce these inconsistencies in the measurements as much as possible, they have been performed multiple times and then averaged. This averaged force response is then used as the force response for that specific pressure combination. The final step for creating the force characterisation is to perform a polynomial fit on this data. More insight into how exactly this characterisation is performed, along with figures showing the results, can be seen in Section 4.2.1.

3.2.2 Using Characterisation as Feed-forward

As aforementioned, this force characterisation will be used in the model as a feed-forward controller. This is realised in the Simulink model in two simple steps. First the controller will check in which discretised pressure region the system is operating. This is done by first taking in the desired force. Then using the previously made polynomial fits to calculate the corresponding positions for each discrete pressure. Using the current measured position together with the calculated positions, the controller can determine in which sub pressure range it is operating. This tells the controller that the pressure needed, to realise the desired force, should be within this pressure range. Simply outputting a constant value per sub pressure range will lead to sudden pressure changes as the handle is moved through the workspace. To determine the output pressure, within the smaller pressure range, a linear interpolation is made between each discretised pressure. The Simulink model implementing this feed-forward controller can be seen in Figures 3.6 and 3.7.

3.2.3 Force Feedback Control

The feed-forward controller, described in the previous section, serves as a first estimate at force control. The force characterisation, that the feed-forward controller is based on, is lacking various dynamics that are not modelled. Additionally, the measurements performed to create the force characterisations are subject to human errors. A feedback controller will be added in order to circumvent having to model all these complex unknown dynamics. This feedback controller will be able to adjust the control inputs of the feed-forward controller, in order to account for its potential inaccuracies.

Since the goal is to avoid having to model the complex dynamics of the system, a model-free control strategy will be used. As described in the literature review (Section 2.1.4), a commonly seen control strategy is a PID controller. In this type of control scheme, the signal to be controlled is measured and fed back to be compared to its desired value. This is the error signal of the system. The error signal is used in different ways to give a corrective input into the system. The different parts of this control scheme are: proportional, integral and derivative feedback, which will be described below.

Proportional Feedback

The simplest part of the feedback controller is the proportional term. It simply multiplies the error signal with the constant K_P and outputs this to the system. This proportional term is shown in Equation 3.3.

$$u_P = K_P (F_d - F_m) \tag{3.3}$$

With:

- u_P: control signal from the proportional term
- K_P: scaling factor of the proportional term
- F_d: desired force [N]
- F_m: measured force [N]

In most control scenarios, this is already able to achieve some level of control over the system. However, in this control scenario, the force being felt at the end-effector needs to be controlled. This force is controlled directly by adjusting the pressure inside the pneumatic actuators. This means that when there is a large error, the proportional term of the controller will also give a large corrective input to the system. This corrective input will adjust the force felt at the end-effector and in turn reduce the error. This result, in a vacuum, is very desirable. However, the proportional term is directly dependent on the error signal. Meaning that the proportional corrective input would decrease and completely disappear when the error goes to zero. This behaviour would still be perfectly fine in most common control scenarios. This system, however, directly controls the force. So, when the corrective input given by the P-feedback term disappears, the system will go back to its original state before any control happened. Implying, that in this scenario, a P-feedback on its own will not control the signal to its desired value. The error signal will settle somewhere between the starting error and zero error. How the force reacts to pressure inputs and the tuning of the P term will determine where it settles exactly.

Integral Feedback

The integral term of the PID controller works differently compared to the proportional term. The integral term integrates the error signal with respects to time. Simply put, this term will accumulate the error over time. This accumulation is then scaled by multiplying it with K_I. This behaviour is shown in Equation 3.4.

$$u_I = K_I \int_0^t (F_d - F_m(t))\, dt \tag{3.4}$$

With:

- u_I: control signal from the integral term
- K_I: constant scaling factor of the integral term

The major benefit of the I-feedback term, is that it is able to hold its corrective output even when the error decreases. When the error decreases, the I-feedback term still has all the previous error signal saved as an accumulation. For that reason, the I-feedback term will be the main driver of the controller's ability of reaching the desired force.

The proportional term is not completely without its use. The integral term will be able to control the error signal to zero. However, it is an inherently slow reacting controller thus will react poorly to sudden spikes in error. A set-point change or sudden movement of the end-effector could cause this sudden spike in error. With only an integral controller, it would take time for the error to accumulate. Meaning it takes time for the integral controller to react. This is where the benefit of the proportional term comes in, since it can react faster to the sudden error spike. In turn giving the integral term time to ramp up and take over from the proportional term.

Derivative Feedback

The derivative term is the final main part of the feedback controller. The implementation of this term is slightly different than the commonly seen implementation. Normally, the derivative works on the error signal. Instead, this term will work on the measured force directly. The derivative term can be seen in equation form in Eq. 3.5.

$$u_D = K_D \frac{dF_m(t)}{dt} \tag{3.5}$$

With:

- u_D: control signal from the derivative term
- K_D: constant scaling factor for the derivative term

The reason for this change in implementation, is that the intended use is slightly different. The main use for this term is to counteract the overshoot encountered in later experiments. It accomplishes this by counteracting the rate of change seen in the force measurement. Having the derivative try working on the error signal means sudden set-point changes are included in the derivative. Resulting in very large output spikes.

3.3 Final Controller Model

This section gives an overview of the main Simulink model that generated the results in this thesis. Each section of the model is shortly explained. There are two versions of the model. Namely the initial preliminary model shown in Figure 3.6, which generated the results shown in Section 4.2.2. From these preliminary results several additions were made, resulting in the final force control model shown in Figure 3.7.

The preliminary force controller model in Figure 3.6 is made in Matlab Simulink. The model is divided into multiple smaller coloured rectangles, highlighting the different parts of the model.

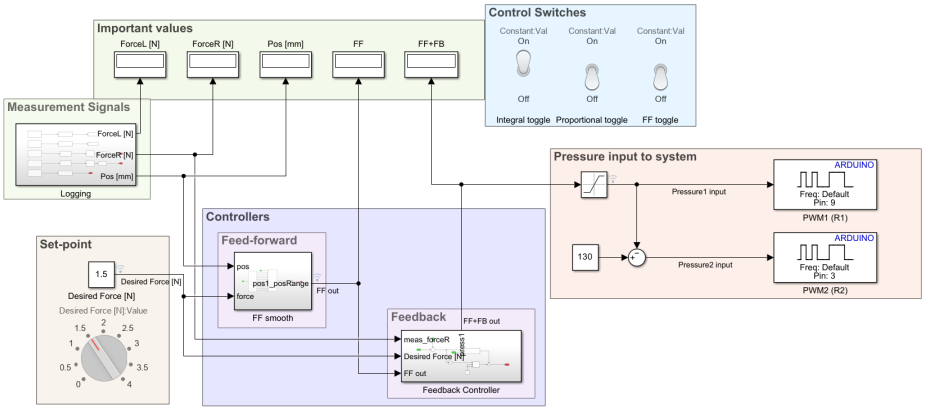

Figure 3.6: Preliminary force controller model in Simulink.

First, the straightforward parts are explained. The light blue rectangle contains the control switches. These switches simply turn on or off specific parts of the controller. The light green area connected to the switches contain display blocks. These blocks are used to show important signal values without having to manually create plots. The set-point section is also self explanatory. It creates the set-point signal and can be changed by using the rotary switch below it.

Subsequently, the measurement signal section, above the set-point, is where the measured signals from the Arduino come in. These incoming signals are then either filtered or changed to units that make sense.

The controller part is the largest element in the model. This section contains the feed-forward and feedback controller subsystem blocks. The feed-forward takes in the force set-point and the current position of the handle-block. It uses these signals to make a first estimation at the desired pressure, using the characterisation made in Section 3.2.1. How this estimation is made, is described in more detail previously in Section 3.2.2. Figures of this subsystem can be seen in Figure A.1.

The feedback subsystem takes in: the measured force, the set-point force and the feed-forward output. These first two signals are used to calculate the error signal. This error signal is then used for the proportional and integral term. The proportional term simply multiplies a constant with the error signal. The integral, however, is slightly more complicated. The accumulative integral has to be limited as to not be able to accumulate outside the pressure range of the system. If the integral is not limited in this way, it can keep accumulating error outside the range. This would be problematic when the error changes sign. Before the integral controller can start reacting to this error, it has to spend time removing all the extra accumulated error. These limits of integral accumulation are dependent on the feed-forward output. The size of the adjustment the feedback can make to the feed-forward, depends on the output of the feed-forward. Figures of the feedback subsystems can be seen in Figures A.2, A.3 and A.4.

Lastly these feed-forward and feedback outputs are added together, which form the pressure input to the right actuator. The pressure of the left actuator is calculated using Equation 3.2.

Two additions were made later on, due to preliminary results produced by the model described above. These two additions are: a limiter on how fast the pressure input is allowed to change and a damping term in the feedback controller. The overview of the final model can be seen in Figure 3.7.

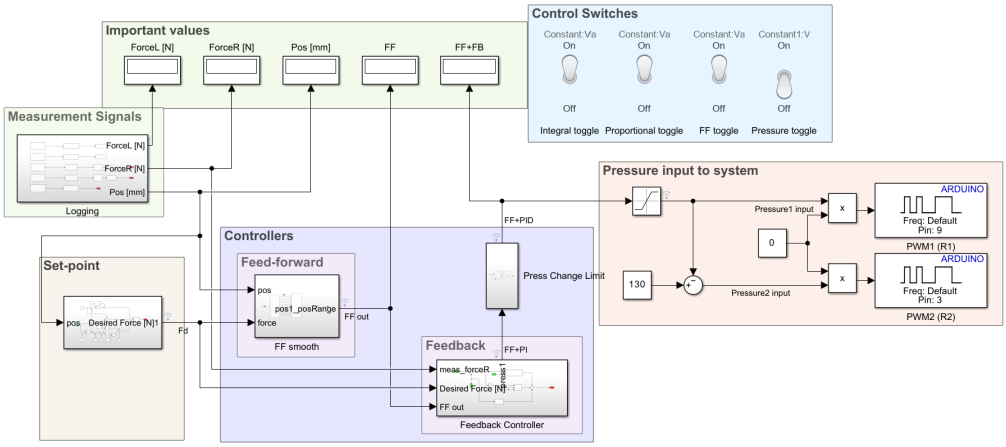

Figure 3.7: Final controller model including the additions based on the preliminary results generated by the model in Figure 3.6.

The first addition is the Press Change Limit subsystem block. This block will act as a limit to how fast the pressure input is allowed to change. It accomplishes this by comparing the current pressure input with the pressure input given in the previous time-step. Limiting this number will only allow the pressure input to change a set amount and act as a speed limit. The inside of this subsystem can be seen in Figure A.5.

The second addition is the damping term inside the feedback controller subsystem block. The measured force is differentiated and then multiplied by a scaling factor, before being combined with the other feedback control signals.

Finally, the set-point creation has been altered. In this subsystem block the realistic force profile is created, which is dependent on the position. This realistic force profile is meant to mimic a needle insertion and is described in more detail in Section 4.2.3.

3.3.1 Tuning Strategy

As mentioned in the previous section, there is a clear distinction made between the first preliminary model shown in Figure 3.6 and the final model in Figure 3.7. This holds true for the tuning strategies as well. First, the tuning strategy used for the preliminary model is explained in detail, followed by the strategy applied to the final model.

The preliminary controller consists of a feed-forward and a PI feedback controller. The parts that need to be tuned are: the proportional and integral terms. Each term of the feedback is responsible for a distinct part of the control action and will be tuned for these situations specifically.

First the proportional term is tuned. This term is responsible for dealing with large sudden spikes in the error. The proportional term is tuned by doing set-point changes in order to mimic these large error spikes. From measurements performed by Gudmundsson it shows that the axial force on the needle can be expected to increase by approximately 0.5N. The set-point change used for the proportional term tuning is set at 1N as a preemptive measure for worse scenarios.

The sequence of events for one of these tuning measurements proceeds as follows. First, the handle is locked in place at the desired position of tuning. This position is kept as constant as possible in order to make the measurements consistent and repeatable. After the handle is locked in place, the system is turned on with a specific force set-point. Only the feed-forward controller is turned on in this scenario. When the system has settled, a switch is flipped which increases the set-point by 1N and turns on the feedback controller. The feedback controller is turned off before the set-point change to make the tuning measurements as consistent and repeatable as possible. Having the P-feedback active before the set-point change causes each measurement to have a different starting point, since the proportional term is different each measurement.

This tuning measurement is repeated for different values of the K_P parameter. The K_P value is increased until it is able to take care of 75% of the set-point change or no significant changes in performance are observed. The 75% rule is not set as a strict rule. The main goal of the proportional term is to take care of a large part of the error spikes. Using 75% of the set-point change will guarantee this.

Next, the integral term will be tuned for the same 1N set-point change. The sequence of the integral tuning measurements proceeds as follows. The handle is again locked in place keeping the position constant. Next, in contrast to the P tuning, both feed-forward and feedback controllers are turned on from the start. After the system has settled on the current set-point, a switch is flipped increasing the set-point by 1N. Most of this error spike will be taken care of by the proportional term. The remaining 25% is for the integral. This tuning measurement is repeated for different values of the K_I parameter, until the control time is within 0.5s or there are no significant changes in performance.

This tuning fully tunes the feedback parameters for a set-point change. This, however, is not the only scenario the controller needs to deal with. The controller also needs to be able to control the force while the handle-block is moving. Extra experiments are performed in order to test and tune the parameters further for movement. In these experiments the set-point will

be constant, however, the handle is slowly pushed through the workspace. These experiments are initially done with the parameters found in the set-point tuning measurements. Parameter values can still be slightly modified to compromise on the set-point change performance, but increase performance during movement.

The next step to tuning and testing the preliminary model, is to test it on a realistic needle insertion force profile. The results from this test is what led to the addition of the previously mentioned damping term and pressure change limiter. This realistic needle insertion force profile is not created with data but uses the results of Okamura, Simone and O'Leary (2004) to create and mimic this force profile.

Implementing this force profile revealed that the most difficult behaviour to control will be the initial puncture of the tissue. This puncture causes a very sudden drop in force and is very similar to the set-point change used in the previous tuning. The difference is, that it is a set-point drop instead of an increase. This means that for these tuning measurements a set-point drop of about 1N will be used instead.

The previously tuned parameters will be kept the same, since they showed really good performance. This means only K_D and the maximum pressure rate of change need to be tuned. As mentioned, this will be done with a set-point drop instead of an increase. Apart from this change the tuning experiments will be the same. The handle will be locked in place at the desired position. Then the controller will be turned on. Once the controller has settled on the set-point the set-point is dropped by 1N.

Similar to the preliminary model's tuning, the introduction of movement and human interaction significantly affected the controller's performance. Due to this, numerous experiments will be performed both with the handle locked in place and with the handle moving together with the realistic force profile.

3.4 Actuator Degradation

As previously mentioned, the main difficulty of working with this system lies in the choice of actuators. The actuators show non-linear and hysteretic behaviour. Adding to these challenges is the actuators' degradation over time. This means that the way the actuators respond to a specific pressure change will be different depending on usage and age. Taking this behaviour into account for the controller is outside the scope of this thesis, however, some research is done into how much the actuators change over time.

Both of the feed-forward controllers are the most affected by this degradation. For both of the feed-forward controllers some form of system characterisation is necessary, which is logically affected by the changing actuators.

To gain insight in the effect of the degradation on the position control, the tuning measurements have been performed regularly over the life span of the actuators. This will give insight into how the feed-forward parameters change due to actuator degradation.

Gaining insight into the effect of degradation on the force control feed-forward is more complicated. The measurements required for this characterisation are time consuming. This means that performing that set of characterisation measurements numerous times throughout the life span of the actuators is not feasible. Instead the final characterisation plots (e.g., Figure 4.4) for different actuator combinations will be compared to each other. This should give some insight into how much variance in behaviour can be expected between different actuators.

4 Results

In this chapter, the results of all the experiments discussed in Chapter 3 will be shown. Section 4.1 is dedicated to the experiments comparing the new actuation method to the old one. First, the results of the backlash tests are shown, followed by the comparison of the force reduction for both actuation methods.

Section 4.2 contains the results of the force control efforts. Firstly, the resulting force response characterisation, which is used as a feed-forward controller, is shown. Secondly, the tuning results of the preliminary PI controller are showcased. Along with its force control performance with a constant set-point. Section 4.2 ends with the implementation of the realistic needle insertion force profile and the force control performance of final model, as discussed in Section 3.3.

Finally, Section 4.3 consists of the results of the actuator degradation experiments, as discussed in Section 3.4. This section comprises of two parts. Initially, the effects of the degrading actuators on the parameters of the position controller are shown. In the following part, the same will be done for the feed-forward force controller.

4.1 Actuation

The feed-forward position controller was tuned with both actuation methods. The first evaluation experiments, as mentioned in the comparison experiments (Section 3.1.2), are the backlash tests. The results of the coupled and uncoupled actuation methods can be seen in Figures 4.1 and 4.2, respectively.

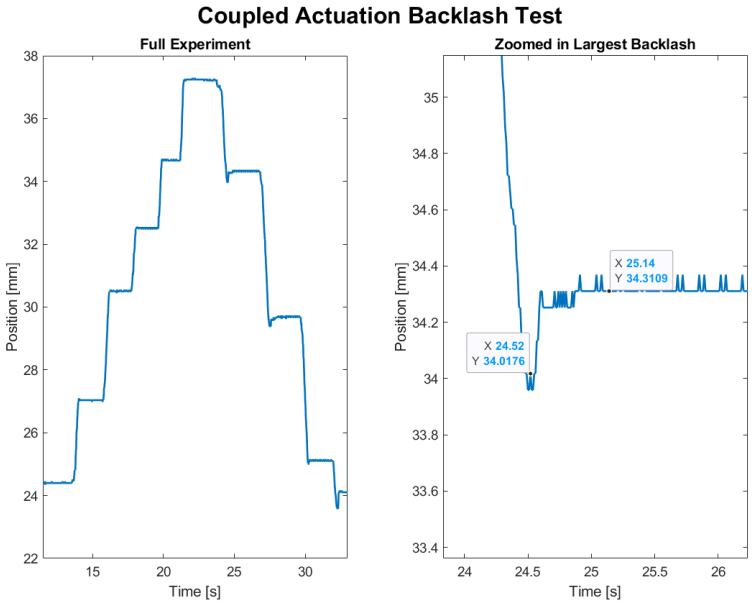

Figure 4.1: Coupled actuation method backlash experiment. (Left) Full experiment result. (Right) Zoomed in version of the largest backlash in measurement.

In these experiments, the handle is moved in both directions through the entire workspace while suddenly letting go of the handle at several positions. The full measurement run can be seen in the left plots. The figures on the right are a zoomed in version of the largest backlash in that measurement along with data tips showing the values. The largest backlash experienced

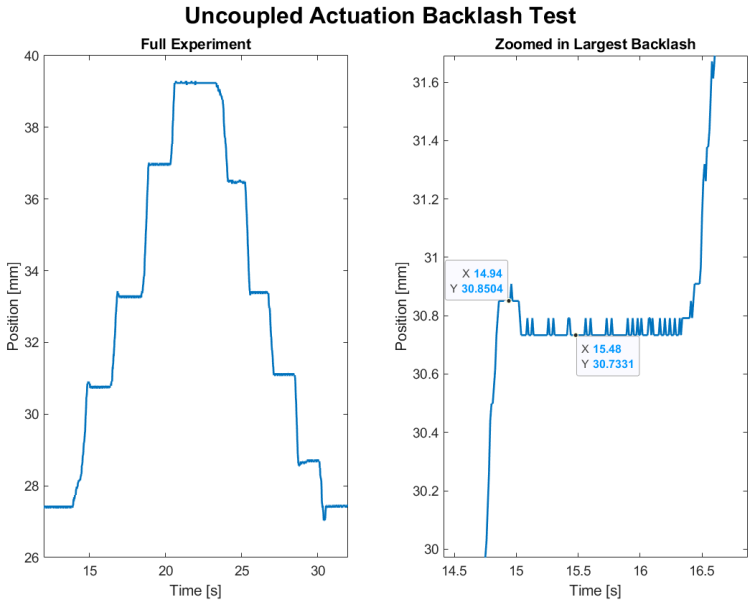

Figure 4.2: Uncoupled actuation method backlash experiment. (Left) Full experiment result. (Right) Zoomed in version of largest backlash of measurement.

in the coupled method is approximately 0.29 mm. The largest backlash using the uncoupled actuation is around 0.12 mm.

The second experiment is comparing the force requirement for movement throughout the workspace, for both actuation methods. In the experiment, the handle is pushed back and forth multiple times, while trying to avoid exceeding the workspace. Judging where the workspace ends is quite difficult and led to several pushes exceeding the workspace. This explains some of the sudden higher force peaks. The resulting peak force ranges in the experiments are summarised and listed in Table 4.1. This clearly shows the effect of the position controller. More detailed plots of these measurements can be found in Appendix A.3.1.

	Left Forces [N]	**Right Forces [N]**
Coupled	[0.27 0.39]	[0.49 0.58]
Uncoupled	[0.21 0.28]	[0.53 0.67]
No controller	[3.16 3.67]	[4.88 5.24]

Table 4.1: Table of the peak force ranges for each actuation method and direction of movement from the experiment previously discussed. The results without any control are also added as a reference. More detailed data shown in Appendix A.3.1

4.2 Force Control

This section is dedicated to the force control results. First, the results of the characterisation of the system's force response is shown in Section 4.2.1. This is followed by the tuning and control performance of the preliminary PI controller in Section 4.2.2. Finally, the resulting needle insertion force profile is shown together with the force control performance of the final controller (Section 4.2.3).

4.2.1 System Characterisation

The measurements for the system characterisation have been performed as described in Section 3.2.1. The multiple measurements per pressure input combination are performed within the same experiment. It is done by slowly letting go of the handle. When all applied force is removed a new push is started. An example result of one of the characterisation measurements can be seen in figure A.9.

As shown in Figure A.9, five push measurements have been performed per pressure combination experiment. These measurements are later split up using a corner detection algorithm. This algorithm finds the start and end point of each push and release measurement, which is then used to split up the data from the entire experiment. For a more in-depth look at the corner detection algorithm, a pseudo code explaining the algorithm is included in Appendix A.1.3. Performing all the measurements within one experiment significantly cuts down on the total time necessary to perform all the characterisation measurements.

The five push force responses are then averaged into one force response. The result for one of the discretised pressure combinations can be seen in the left plot of Figure 4.3. The right plot in Figure 4.3 shows the resulting averages for all the different pressure combinations, along with their corresponding standard deviations.

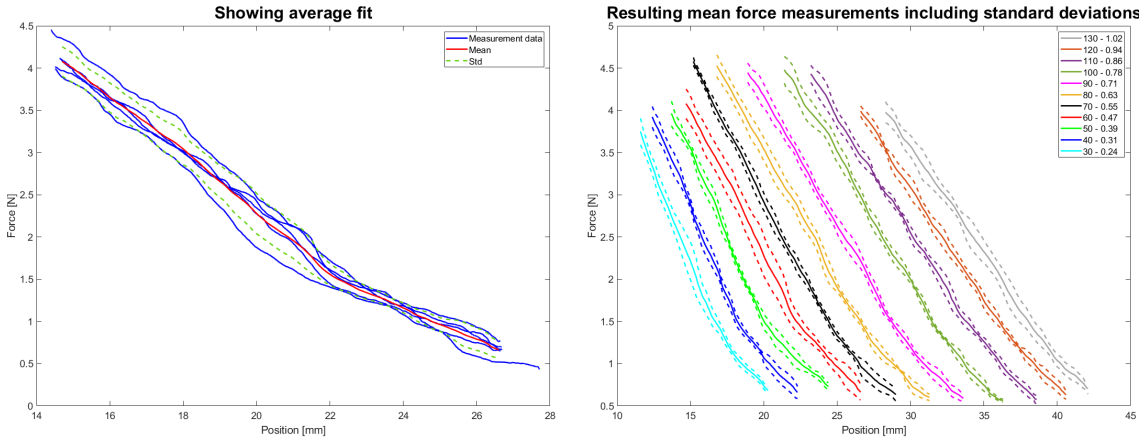

Figure 4.3: (Left) Showing the five push measurements together with the mean force response and standard deviation. (Right) Mean force response with standard deviations for all discrete pressure combinations.

The data shown in the right plot of Figure 4.3 will be used as the main force characterisation of the system. This will serve as a first feed-forward estimate for the pressure that is necessary for the desired force. To do this a polynomial fit has been made on the force response for each discrete pressure. These polynomial fits have been made using the Matlab function polyfit.

Multiple degrees of polynomial fits have been made on the data. A quadratic polynomial resulted in an accurate fit, while increasing the degree further did not improve the quality significantly. Pseudo code of the entire data processing algorithm can be found in Appendix A.1. The polynomial fitting results can be seen in Figure 4.4.

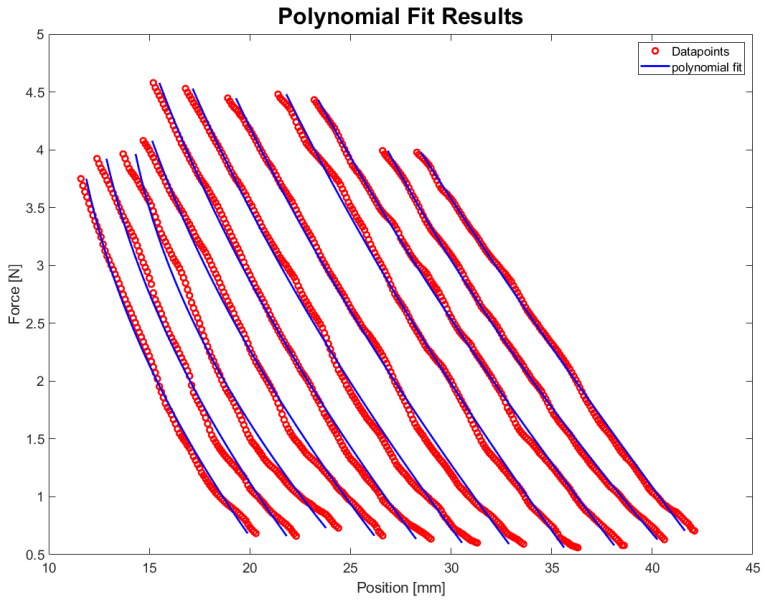

Figure 4.4: Resulting quadratic polynomial fits on the characterisation data.

4.2.2 Preliminary PI Tuning & Control

The proportional set-point tuning results can be seen in Figure 4.5. An important thing to note for the plot of this result, is that the set-point change was activated manually. This meant that the timing of these set-point changes are in reality not lined up. The measurements have been aligned manually. This clearly show the difference in performance between each value of K_P.

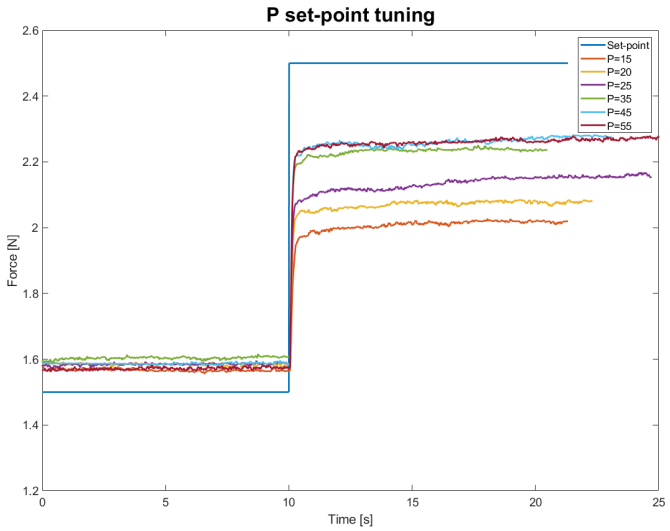

Figure 4.5: Proportional set-point tuning for different P parameters.

From the tuning measurements shown in Figure 4.5, it can be seen that after a K_P value of 35 no significant change in performance occurs. This means that $K_P = 35$ is taken and used for the integral set-point tuning.

The results of the integral tuning measurements can be seen in Figure 4.6. The same note has to be made as with the proportional set-point tuning. The time axes has been shifted to align the measurements for easy comparison.

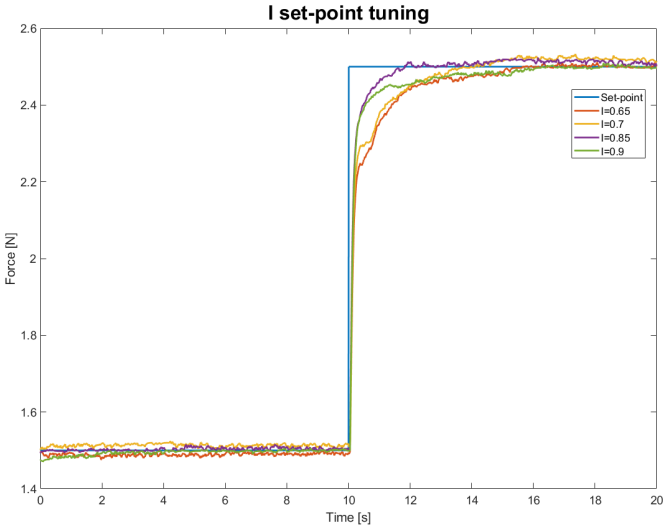

Figure 4.6: Integral set-point tuning for different I parameters.

These tuning experiments show that both $K_I = 0.85$ and $K_I = 0.9$ satisfy the control time requirement. However, the performance with $K_I = 0.9$ is slightly slower than with $K_I = 0.85$. This means that the optimal value for K_I is taken as $K_I = 0.85$.

Next up are the results of the control performance during movement with a constant set-point. The results can be seen in Figures 4.7 and 4.8. These two experiments show two different movements. In Figure 4.7, the handle is moved through the entire workspace in one direction. Figure 4.8 uses less movement but changes direction halfway through.

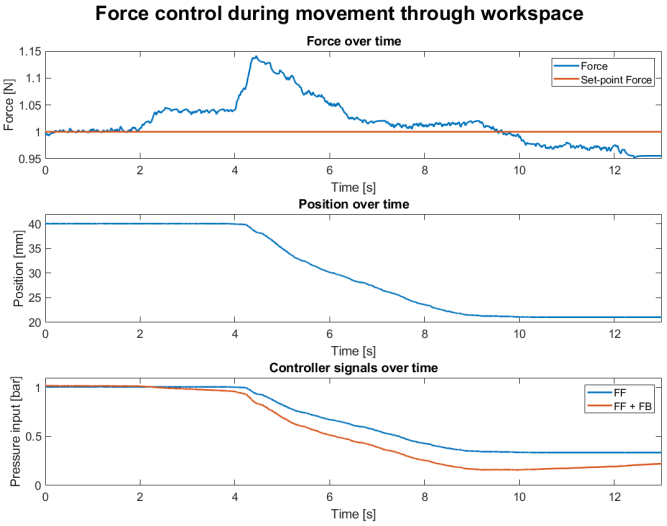

Figure 4.7: PI force controller performance after set-point tuning. Handle is moved from one end of the workspace to the other. A constant force set-point of 1N is used.

As can be seen in the figures, the performance in both scenarios is quite similar. The full range movement shows a peak error in the force of $0.15N$ and the double direction movement a peak of $0.2N$. For both movements, the force error after the initial peak does not exceed $0.05N$.

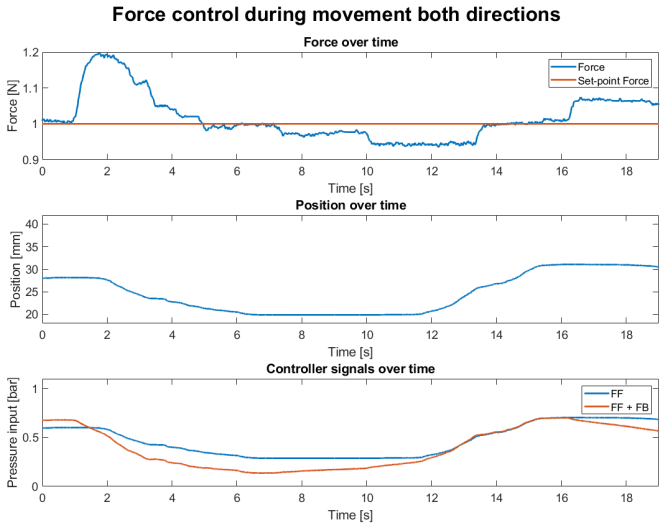

Figure 4.8: PI force controller performance after set-point tuning. The handle starts in the middle and is moved to the end of th workspace and back. A constant force set-point of 1N is used again.

4.2.3 Final Control with Realistic Force Profile

The first step, needed to produce the results, is to create the realistic force profile based on the results from Okamura, Simone and O'Leary (2004). The tissue puncture data shows a significant amount of variance between experiments. This is largely due to the stiffness variations in the tissue. Okamura, Simone and O'Leary have data from two different livers. One of which is significantly stiffer than the other. The data from the stiffer liver is used as a worst case scenario. Additionally, using a stiffer tissue allows the force profile to fit within the rather limited workspace, while leaving room for the cutting and friction behaviour.

The cutting and friction behaviours have been recreated using a linear relation between the position and force. The results shown in Figure 2.3 have been used as an indication for typical force values in this scenario. The resulting needle insertion force profile can be seen below in Figure 4.9.

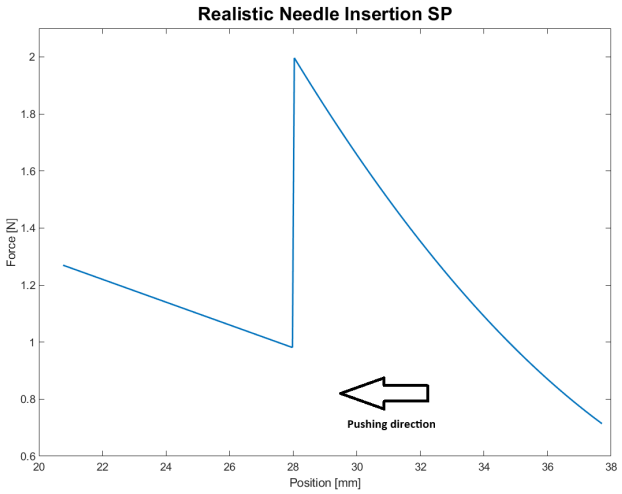

Figure 4.9: Force vs position plot of the mimicked needle insertion profile. Tissue puncture is set here at 28mm.

An important thing to note about Figure 4.9 is that the pushing direction is towards a decreasing position. This is also indicated in the figure to be less confusing.

Next, this force profile is used as a set-point for the PI controller. In this experiment, the user will start in the left most part of the workspace. Once the controller has settled, the user will slowly start pushing the handle. After puncture occurs, the user tries to keep the handle position constant, while the controller regains control. After this short pause, the user will continue pushing the handle through the workspace. The resulting experiment can be seen in the top two plots in Figure 4.10.

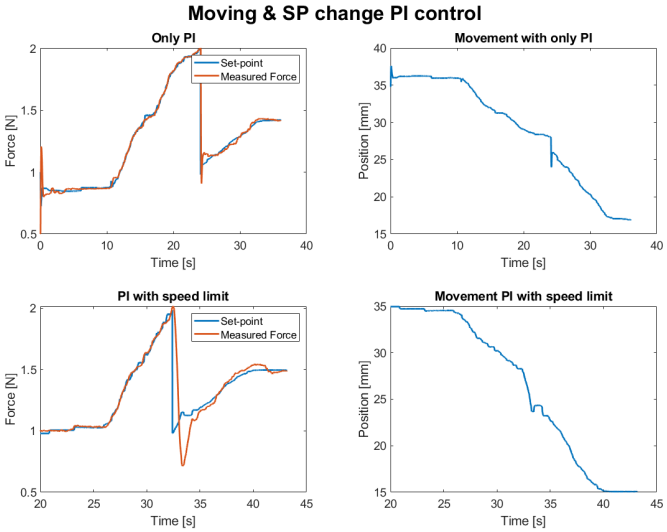

Figure 4.10: Force control performance using Figure 4.9 as set-point. (Top left) Force control with only PI control. (Top right) Movement during force control with only PI control. (Bottom left) Force control with the added speed limit of 0.65. (Bottom right) Movement during force control with speed limit.

As can be seen in Figure 4.10, the control with only PI is very aggressive, which also was an issue in the previous results. Furthermore, this aggressiveness causes a sudden jerk in movement at the puncture set-point change. These observations led to the addition of the speed limit on the input pressure change. As a first estimate, the limit was set at 0.65 pressure change per time step (the time step is 0.01s). This speed limit equates to approximately 0.005 bar per time step. This allows the pressure to go from zero to maximum input in two seconds. The resulting performance can be seen in the bottom two plots in Figure 4.10.

Figure 4.10 shows that adding a speed limit increases the overshoot significantly and, as expected, increases the time it takes to regain control. To improve these performance measures the damping term was added to the feedback controller. Numerous combinations of these two parameters have been tested. The two best performing combinations that were observed, are shown in Figure 4.11. The overshoot, along with control time of these two parameter combinations, are listed in Table 4.2. The performance measures of Figure 4.10 are also shown in this table.

(SL,K_D)	Overshoot [N]	Control Time [s]
(0,0)	0.2	0.19
(0.65,0)	0.44	1.67
(1,6)	0.19	1.96
(1.25,6)	0.19	1.47

Table 4.2: Performance results of experiments shown in Figures 4.10 and 4.11. SL stands for speed limit.

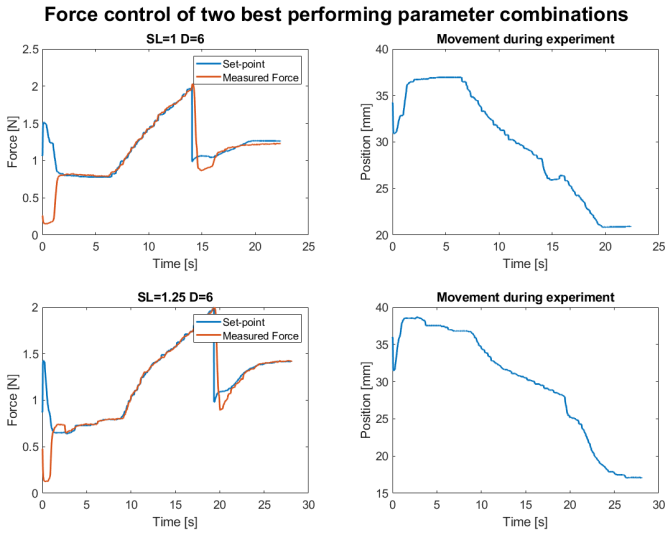

Figure 4.11: Force control results showcasing the two best observed parameter combinations.

The second experiment tunes the speed limit and damping parameters. In this experiment, the inconsistencies caused by human interaction with the system are removed by instead locking the handle in place, similar to previous tuning experiments. While being locked in place, the handle will be subjected to a 1N set-point drop around the same position as the tissue puncture in Figure 4.9(at around 28mm). The two best performing parameter combinations are shown in Figure 4.12. Table 4.3 shows the overshoot and control time performance for these parameter combinations. The two top performing parameters from the previous experiment and a low speed limit with zero damping are also included as reference.

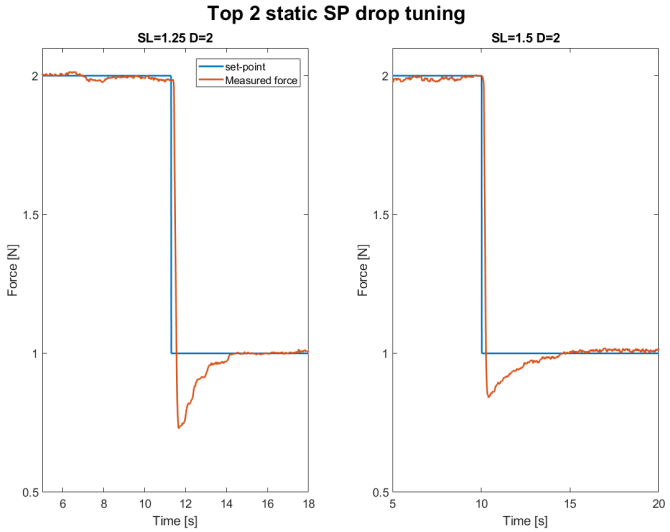

Figure 4.12: Static set-point drop results showing the two best performing parameter combinations.

(SL,K_D)	Overshoot [N]	Control Time [s]
(0.65,0)	0.43	2.03
(1,6)	0.33	1.74
(1.25,6)	0.31	1.71
(1.25,2)	0.27	1.37
(1.5,2)	0.19	1.14

Table 4.3: Performance results of the static set-point drop tuning

4.3 Degradation Results

As discussed in Section 3.4, the position control feed-forward tuning measurements have been repeated multiple times over the life span of the actuators. The tuning of this feed-forward controller consists of two linear fits, each with a slope and an intercept. These tuning measurements were performed twice, back to back, on each measurement day. This was done to simply have more measurement data and have some form of back up data in case something went wrong. In one of these measurements, the pressure input sinusoid (Figure 3.2) was given as input to the system for 100 seconds. The linear fits of the feed-forward controller only require one full period of this input sinusoid. The feed-forward parameters were calculated for multiple different periods, since 100 seconds gives multiple full periods. Figure 4.13 shows the means and standard deviations of the parameters for each 100 second measurement. The results are split up per day of measurement and whether it was the first or second tuning measurement that day.

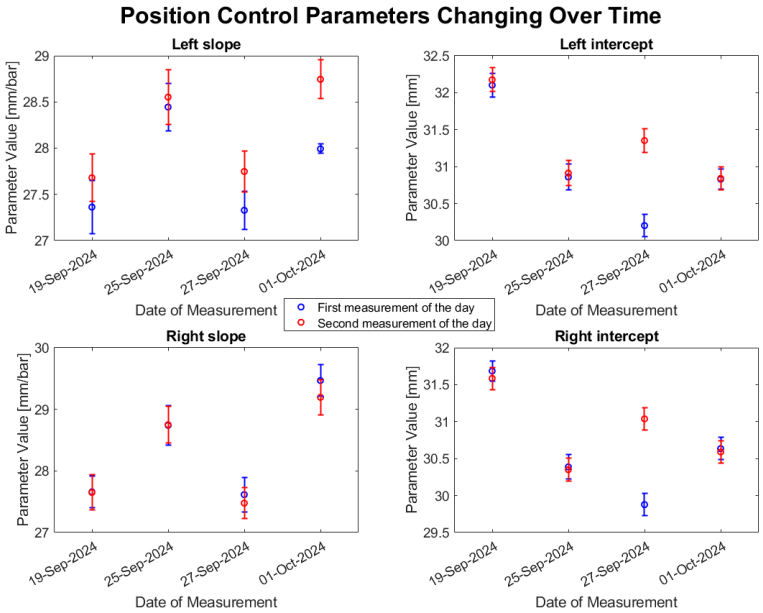

Figure 4.13: Means and standard deviations of the feed-forward position control parameters. Results are split up per day and per measurement of that day.

Figure 4.14 shows and compares three different force response characterisations. The characterisations shown in this figure are performed as discussed in Section 3.2.1. Figure 4.14 shows the final results after having performed the polynomial fits. The first characterisation is the blue (top left) plot. This characterisation was done with both completely new left and right actuators. Eventually the right actuator was replaced. The red (top right) plot shows the resulting characterisation with this new right actuator. This new right actuator ultimately had to be replaced again. The green (bottom left) plot is the resulting characterisation with this second new

right actuator. The left actuator was kept the same in all three characterisations. The bottom right plot shows all three force responses together with the same colour distinction.

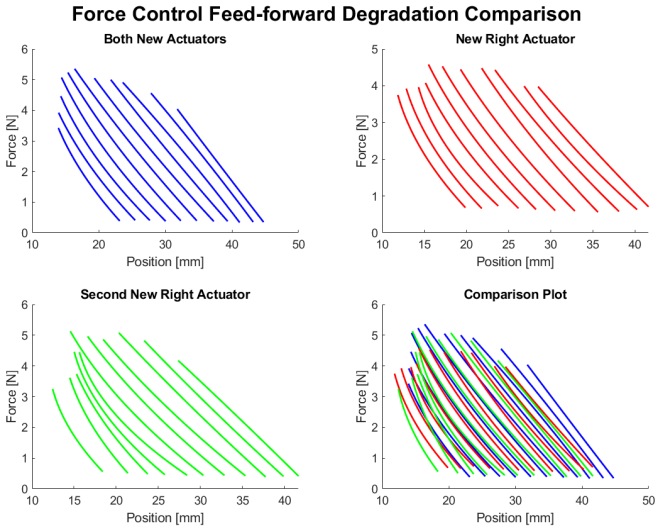

Figure 4.14: Three different force response characterisations. Each characterisation uses a different right actuator. Bottom right plot shows all three characterisations together for comparison.

5 Discussion

In this chapter, the results showcased in the previous part are discussed in more detail. Furthermore, issues encountered while working on the system are highlighted together with their effects on the results. First, the results from the proposed actuation method are discussed (Section 5.1). Next, the force control results of the preliminary model are analyzed, together with the main problems faced during those experiments (Section 5.2). This is followed by a discussion about the mimicking of a realistic needle insertion force profile (Section 5.3). This section also further analyses the results of the final controller model using this realistic force profile. The actuator degradation results are discussed in more in detail in Section 5.4. The final section discusses more general problems encountered with the system (Section 5.5).

5.1 Actuation Methods

The first results to be discussed are the position control results with a coupled antagonistic actuation method. The results can be seen in Section 4.1. The main goal of this new actuation method is to simplify the force control in the later parts of the thesis. The important question regarding this actuation change is, how would it affect the position control performance? The most important result is the backlash test, since this will be the main function of the position controller in the final system. The largest backlash for the coupled method is more than twice as large as the uncoupled actuation method. This result sounds worse than it in reality is. The absolute value of both methods are small enough to be practically unnoticeable while using the system. Nevertheless, the larger backlash observed with the new method could still cause unwanted needle movement. This potential issue is very easily avoided by having the force and position control fully separated in the complete system. This separation means that the position control should only be active when the user lets go of the handle and no movement is happening. This allows for the needle to be locked in place when the controller is in position control mode.

The force reduction test, as mentioned in Section 3.1.2, is mainly carried out for comparison purposes. Looking at the forces needed for movement for both actuation methods, shows that the performance is quite similar. The coupled method is slightly better while moving to the right and the uncoupled method is slightly better in the left direction. There is, however, a significant difference in the forces between movement direction for both actuation methods. This is most likely caused by a difference in actuators. The right side actuator had to be replaced more often, which means this actuator is newer and stiffer.

5.2 Preliminary PI Force Control

The force control tuning results showed some unexpected behaviour in the proportional setpoint tuning. Figure 4.5 shows no increase in performance for K_P values above 35. This is unexpected, since a higher K_P value with the same force error should result in a higher pressure output. This, in turn should result in a lower force error. To explain what causes this, an important problem with the system should be explained.

By far the largest issues while working with the system were consistency and repeatability issues. In the beginning, before the bushings of the handle were changed, it was close to impossible to perform consistent and repeatable experiments. There was too much wiggle room in the handle-block, causing the contact point between the handle and the force sensor to be extremely inconsistent. A slight movement, not directly in the direction of intended movement, could cause the force measurement to change drastically. This behaviour is still present after the bushings were changed, however, it is significantly reduced. This increased the consistency and repeatability drastically and made force control possible.

This change came with an unfortunate side-effect, which exposed another design flaw of the system. The handle is located above the force sensors and guiding rail. This means that when the user pushes on the handle, it creates a torque on the bushing and the guiding rail. The combination of the tighter bushings and this extra torque caused the system to have a lot of static friction. The extra friction in the guiding rail was simply fixed by using lubrication. Though, this lubrication did not fully resolve the problem inside the handle-block. This caused the handle to be able get 'stuck' at higher force values. Figure 5.1 showcases this problematic behaviour.

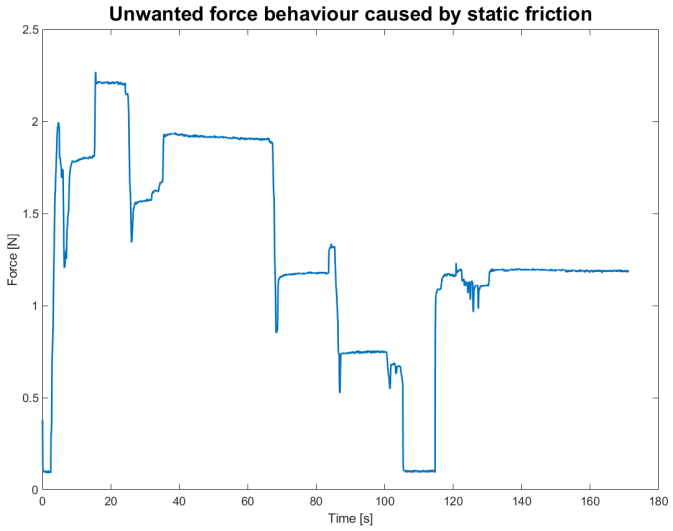

Figure 5.1: Force measurement showcasing the unwanted force behaviour caused by static friction. Position and pressure are kept constant while manually giving small force impulses.

In the experiment shown in Figure 5.1, everything is kept constant. The handle is locked in place and the pressure in the actuators does not change. The only inputs given to the system during this experiment, are short force impulses. These small spikes in force are being applied manually in both directions. If everything was working properly, this short spike in force should be seen in the measurement. Nevertheless, shortly after the force should return to its original value before the impulse. What is happening, however, is that the force does not go back to its original value. This precisely showcases the unwanted static friction produced by the torque problem, together with the tighter bushings. Causing the force to remain at its impulse level. That means the user can manually adjust the force to whatever they want it to be and the force measurement will stay there.

This knowledge explains the previously mentioned unexpected behaviour in the proportional force control tuning. What is actually happening in Figure 4.5 with the P controller, is that the sudden force error gives a spike in pressure. The height of this spike is dependent on the value of the K_P parameter. This spike in pressure is very similar to the force impulses in Figure 5.1. The real reason why it does not improve in performance for K_P values above 35, is that for those K_P values the pressure spike hits the saturation point. This means that increasing the K_P parameter beyond these values does not change the ending force, since the main driver of these large force changes is the height of this pressure spike. Having tuned the proportional parameter in this way, essentially, teaches the controller to exploit this unwanted force behaviour.

If the only goal is to control the signal, then this way of tuning and controlling is acceptable. Due to it being very effective in controlling the signal as shown in the performance results. However, obviously the goal is to control the force experienced by the user and not just the signal. Another major downside to allowing this type of control, is that it will tend towards very aggressive control. This leads to aggressive pressure changes. Aggressive pressure changes

are problematic because this causes the life span of the actuators to decrease significantly. All these control experiments so far have been performed in only one direction. This means that one of the actuators will be mostly subjected to aggressive pressure increases, and the other to aggressive pressure decreases. The actuator subjected to the increases has had to be replaced more than twice as often as the other actuator.

Next up is the performance of the controller during movement with a constant set-point. The main question in this thesis is, whether the controller would be able to keep the force error below the the just noticeable difference (JND) in force. The value of the JND depends on the amount of total force being felt, and how the force is being experienced. Section 2.1.6 mentions the JND for the human finger and the hand with arm. The JND given for the human finger seems quite general, since it is not dependent on the absolute value of the force. Additionally, no information was given on how the force was applied to the finger. Furthermore, the design of the handle of the system seems to suggest it should be operated using the hand with arm. For these reasons, the JND data from Table 2.1 was used instead. In this case, the set-point used is $1N$. The JND for this is not exactly listed. However, with a simple linear interpolation, the estimated JND is approximately $0.2N$. Both the movement experiments are within this requirement. Still, it has to be mentioned that even though this is within the threshold of the JND, it was definitely possible to feel this force spike of $0.2N$.

An important observation from the results shown in Figures 4.7 and 4.8, is that the main sources of error are at the beginning of the movement, and less so shortly after the movement ended. Acceleration is hypothesized as the cause of these two error spikes. When the handle is set into motion, it needs to be accelerated, which requires an extra force. This error spike is partly taken care of by the proportional term, which causes the overall height of the error spike to be decreased. The integral term seems to be too slow to take over from the proportional term. Thus needing time to control the error back to zero. The same explanation can be given for the error shortly after the movement. This theory also explains why the peak error in Figure 4.7 is lower than in Figure 4.8. In the full range movement of Figure 4.7, there is a small increase in force before the movement has started. This allows the integral term to already start accumulating error and in a way 'prepare' itself for the movement that is about to happen.

5.3 Realistic Force Profile Control

After the preliminary PI force control results, the addition of the speed limit and damping term were made. These additions were made together with the introduction of the needle insertion force profile. There is one important note to be made on the mimicked force profile in Figure 2.2. As can be seen, the force profile does not start at zero force. This is done intentionally, since the controller is not able to reach forces lower than 0.5N. Due to the aforementioned issues with the force measurements. This is the only modified and unrealistic part of the force profile. The rest of the force profile still uses realistic force values based on the research done by Okamura, Simone and O'Leary.

After the addition of the speed limit and damping term, two different experiments were carried out to find suitable parameter values. In the first method, the controller is simply subjected to the needle insertion profile. The second method tried to remove the inconsistencies potentially caused by human interaction. This is done by locking the handle movement and only subjecting it to the tissue puncture part of the profile. The tissue puncture part was isolated, since the speed limit and damping are largely exclusively active during this part of the force profile. The interesting result to point out, from these two different methods, is that the observed best parameters are different for each method. This is to be expected to some degree, since the experiments are not the same. However, a large part of this difference can be attributed to human bias. After performing the same experiment multiple times a feeling started to form predicting the tissue puncture.

5.4 Actuator Degradation

First looking at the position control degradation results (Figure 4.13), it does indeed show that the behaviour of the actuators changes over time. This result was expected, however, it is difficult to recognize a pattern in the long term parameter changes. Nevertheless, a pattern did seem to emerge in the short term parameter variations. As explained in Section 4.3, multiple different periods were used to calculate different parameters. The parameter change observed between these periods is, in contrast to the long term variations, very consistent. The left slope, the right slope and the left intercept all steadily increased without exception, as the measurement progressed. The right intercept, however, always decreased as the measurement proceeded. This seems to suggest, that the actuators have some form of 'warming up' period. Looking back at the backlash tests in Section 4.1 with this knowledge, it could very well explain the difference seen in the performance of each actuation method. More research would have to be done into the effect of the parameter variance on the position control performance in order to confidently make this link.

A few key observations were made while looking at the effect of the changing actuators on the force characterisations. Section 5.2 shortly mentions the effect of the controller's aggressiveness on the actuator life spans. This aggressiveness led to only the right actuator being replaced in the three characterisations shown in Figure 4.14. This meant that, in the red and green characterisations, in Figure 4.14, the right actuator is completely fresh. The effect of these series of actuator replacements can be observed in the bottom right plot of this figure. The overall workspace of the characterisation is slowly shifting towards the lower position values. In the physical setup this means it is slowly shifting towards the newer right actuators. This shifting workspace is in line with the hypothesis of the actuators slowly degrading through usage, since the newly made actuator is expected to be stiffer. This stiffer actuator will naturally pull the workspace more towards that side of the movement range. This shift in workspace does seem to suggest some long term degradation effect being present in the actuators. Which contrasts the observed results of Figure 4.13.

The second key notable difference between the three characterisations is that, for the blue plot, the force responses at different pressures are all nicely aligned. This seems to break down slightly for the left most force responses in the red characterisation. The green characterisation makes this break down even more apparent. This much steeper increase in force, is caused by the right actuator starting to buckle. The buckling here, is caused by moving too close to the right actuator. This also explains why the break down is more aggressive in the green characterisation, since its workspace is naturally shifted more in that direction.

5.5 General System Problems

As may have become apparent, this system was not easy to work with. The biggest issues encountered were the problems caused by the inconsistent force measurement and added friction from the new bushings, as discussed in the previous sections. A secondary and more minor issue, was that the system always seemed slightly stuttery. This was largely reduced by adding the lubrication to the guiding rail, however, not completely.

When installing an actuator, the open side of said actuator needed to be very tightly connected. Preventing air leaks from occurring. In the later stages of the research, it was discovered that this tight connection caused the extra material at the entrance of the actuator to be squished together. In the worst case scenario, this caused the entrance to be fully sealed and almost work as a makeshift valve. This excess material at the entrance was later removed. It is difficult to fully know the effects of this, since the pressure sensor is located in the pressure regulator and cannot measure the pressure directly inside the actuator. This makeshift valve could explain some of the stuttery movement observed.

The last notable system issue is its fragility. A significant amount of time was lost to the system breaking down seemingly over night. One of these break downs occurred in the ending stages of this thesis. One of the actuators broke along with the bushings being worn out. The bushings could unfortunately not be replaced in time, which meant the force sensor measurements were not reliable due to the very high static friction of the worn out bushings. This meant that the tuning and testing of the speed limit and damping term parameters was cut short. Additionally, this break down made the experiments in which the effects of actuator degradation on control performance is tested, rendered impossible.

6 Conclusions and Recommendations

6.1 Conclusions

The main question posed in the beginning of this thesis, was whether a model-free controller could deliver precise force feedback using non-linear soft pneumatic actuators suffering from hysteresis. In order to answer this overarching question, several subquestions were posed and explored first.

Firstly, a new actuation method was proposed along with completely separating the position and force controllers. The new actuation method significantly simplified the force control and showed slightly worse position control backlash. The slightly worse backlash is still acceptable, especially with the proposed separation of controller modes. The worse performance could also be explained by the parameter variance observed in the actuator degradation results of Figure 4.13, as discussed in Section 5.4.

Next, the force control performance of a PID controller together with feed-forward was tested in different scenarios. For movement with a constant force set-point, a PI controller with feed-forward was capable of keeping the force error below the JND. After changing the set-point to a realistic needle insertion force profile, the main difficulty came from the large set-point drop at the initial tissue puncture. Overshoots within the JND, caused by this set-point drop, have been observed in both the movement and static control tests. The overshoot experienced seems to be very dependent on how the user interacts with the system during this large set-point change.

The durability and deterioration of the actuators were investigated as well. Definite changes and degradation of the actuators over longer periods of use was observed. Additionally, a secondary effect was observed in which the actuators showed consistent short term parameter changes within measurements. The effect of these parameter variations on the position and force control performance have not been tested directly. However, the force control results have inherently been subjected to degradation, since the characterisation for force control is only performed once at the start of the actuator's life span. This suggests that the force controller is capable of dealing with these changing parameters. Still, more research is required to be able to answer that question in more detail.

The final performance of the force controller seems very promising when looking back at all the results. The main limitation of the system's force sensors has been discussed, along with its interaction with the proportional term. This interaction resulted in an unrealistic performance with sudden set-point changes. Therefore, the performance in these scenarios is inconclusive and needs further research. The force control during constant and gradually changing set-points showed excellent performance. This performance, despite the numerous issues encountered with the system, shows its potential. To that end, it can be concluded that a model-free controller is capable of providing force feedback within the JND, while dealing with the non-linearity and hystersis of the actuators in the case of slow set-point changes.

6.2 Recommendations

Based on the results and experience with the system the following recommendations for future work are made.

6.2.1 System Redesign

Some system redesigns seem quite necessary based on the problems encountered. Most importantly, the method of switching between force sensors needs to be changed. This caused a lot of issues with the reliability of the force measurements. Especially, together with the added torque when pushing on the handle. A suggestion could be removing one of the force sensors

and avoiding the switching behaviour all together. If the goal is only to perform force control during insertion, then there seems no need for the second force sensor.

A second minor recommended system improvement is simplifying the changing of actuators. Currently, depending on which actuator needs to be replaced, the entire system needs to be taken apart in order to change it.

6.2.2 Control During Set-point Changes

Further research is necessary into the force control performance during sudden set-point changes. Before this can be done, the suggested system redesigns would have to be carried out, since the issues from the force measurements is what caused the performance to be inconclusive.

6.2.3 Actuator Degradation

More research needs to be done on the effects of actuator degradation on force control performance. Additionally, more work needs to be done investigating the degradation on its own. The shifting workspace (Figure 4.14) suggests a decrease in stiffness caused by long term use. This has not been observed in the position control tuning experiments. This could be due to the position control parameters being dependent on both actuators.

Acknowledgements

First of all I would like to thank both my supervisors, M. Abayazid and M.S. Selim. Both have shown great help in providing overall guidance for this thesis. A special thanks to M.S. Selim for providing insightful discussions and being available whenever necessary.

A. Gąsienica has been a great help in dealing with the force sensor issues encountered during the research. He made the specially printed bushings used inside the handle-block. Without his help the results shown in this thesis would not have been possible.

Lastly, I would like to thank my partner, I.F.F. Nyengaard. She was always available for discussions and general help in dealing with all the smaller issues encountered during this thesis.

A Appendix

A.1 System Characterisation Pseudo Code

A.1.1 Main Algorithm

Algorithm 1 createForceChar

Load Data
- Load and extract necessary data from each pressure measurement

Data Prep
- Moving average filter on position data
- Cut off beginning and ending of measurement

Splitting the Data
- [push, release] = getData(data)
- Run for each pressure measurement

Create average force responses
- avgForce = getForceFit(pushData)
- Run getForceFit for each pressure

Create polynomial fit
- Use polyfit to create polynomial fit for each pressure force response

A.1.2 getData Function

Algorithm 2 getData(data)

Find corners in position data
- corners = findCorners(positionData)

Split data using corners
- Extract pushing data
- Extract releasing data

A.1.3 findCorners Function

Algorithm 3 findCorners(positionData)

Top cutoff
    - Cutting off the top peaks of the position data
Bottom cutoff
    - Cutting off the bottom peaks of the position data
Find corners in cutoff section
    - Top cutoff corners
        - maxPos = max(posPart)
        - posDiff = abs(maxPos-posPart)
        - find posDiff <= margin
        - corners = first and last entry in posDiff <= margin
    - Bottom cutoff corners
        - minPos = min(posPart)
        - posDiff = abs(minPos-posPart)
        - find posDiff <= margin
        - corners = first and last entry in posDiff <= margin
sort corners

A.2 Model Subsystem Figures

A.2.1 Feed-forward Subsystem

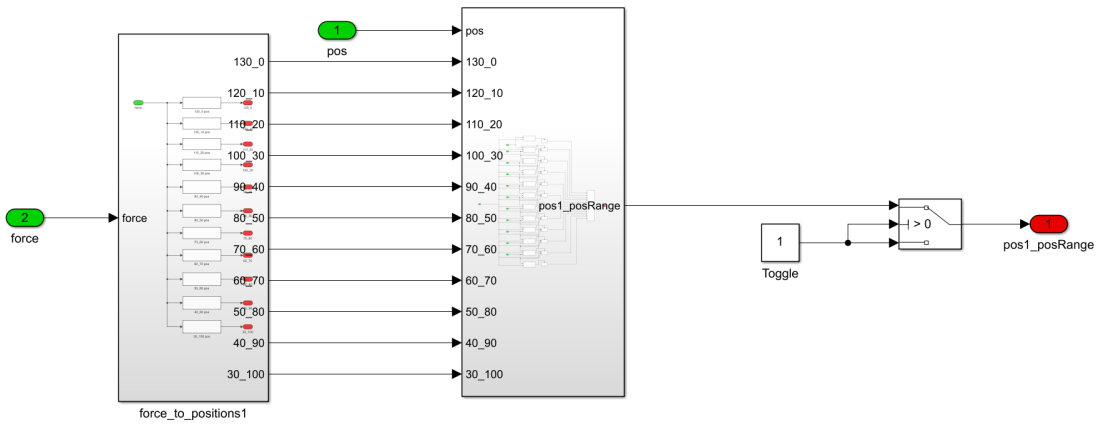

Figure A.1: Screenshot of the inside of the FF smooth subsystem block in Figure 3.6. Further inside subsystems are not shown. Their working is described in Section 3.3.

A.2.2 Feedback Subsystems

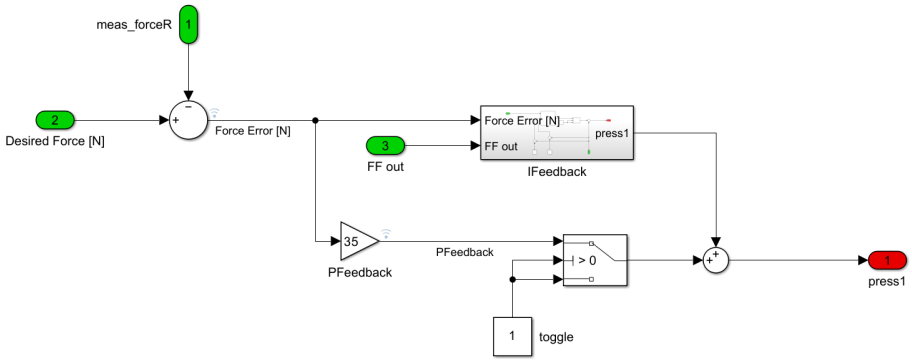

Figure A.2: Screenshot of the inside of the Feedback Controller subsystem block. The inside of the IFeedback block can be seen below in Figure A.3.

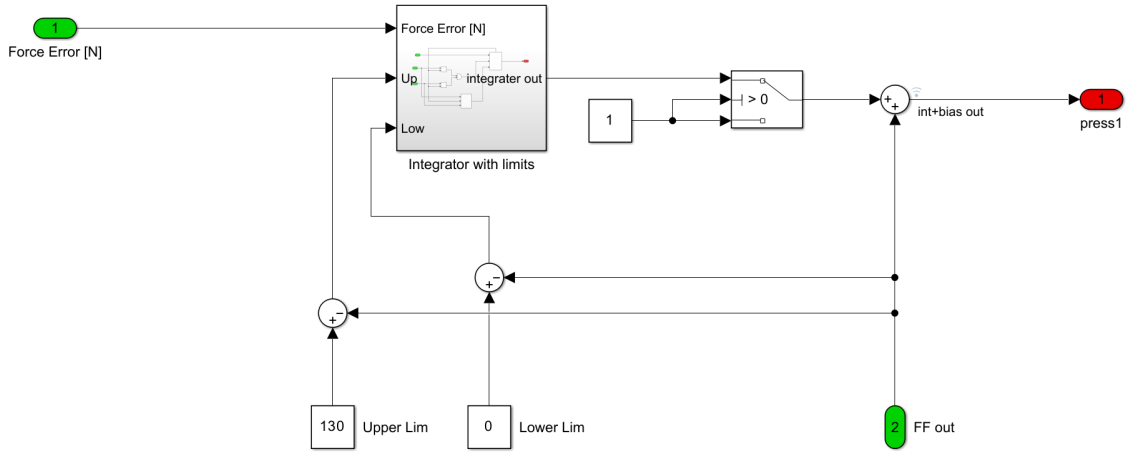

Figure A.3: Screenshot of the inside of the IFeedback subsystem block. The inside of the Integrator with limits block can be seen in Figure A.4

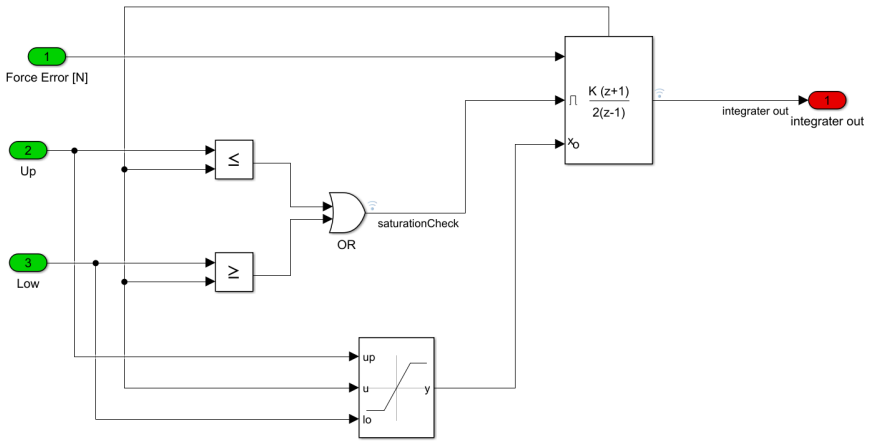

Figure A.4: Screenshot of the inside of the Integrator with limits subsystem block.

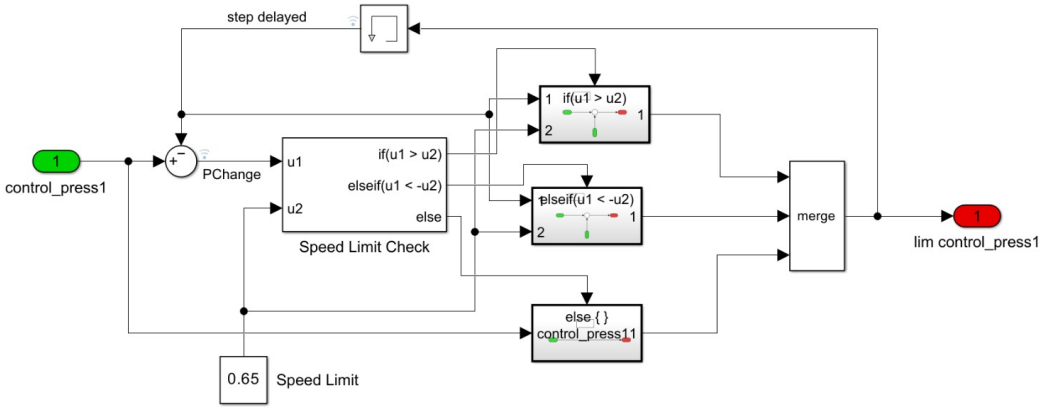

Figure A.5: Screenshot of the inside of the Press Change Limit subsystem block.

A.3 More Detailed Results

A.3.1 Position Control Comparison

The detailed force reduction results, summarised in Table 4.1, can be seen in Figures A.6, A.7 and A.8.

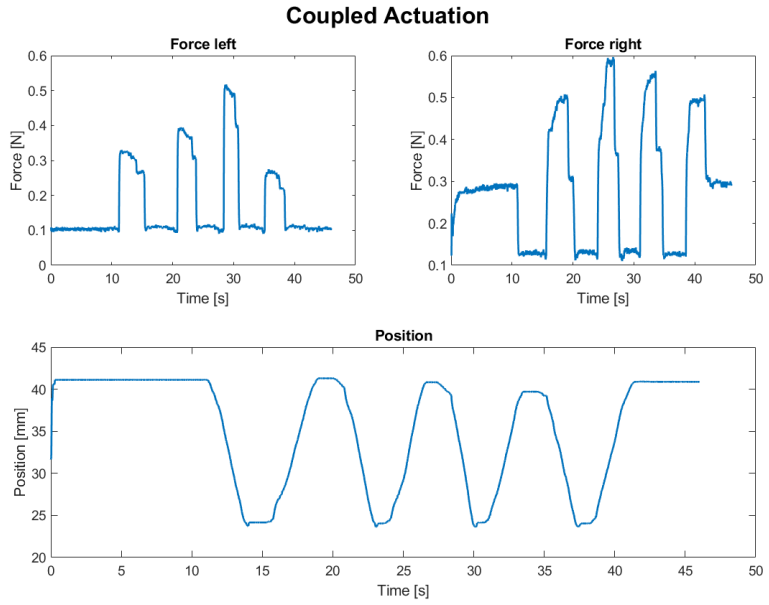

Figure A.6: Force reduction result using the coupled actuation.

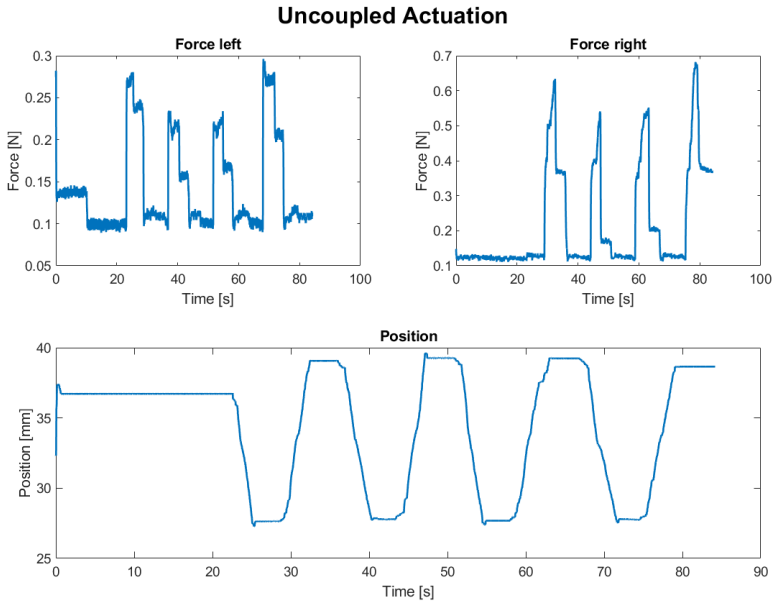

Figure A.7: Force reduction result using the uncoupled actuation

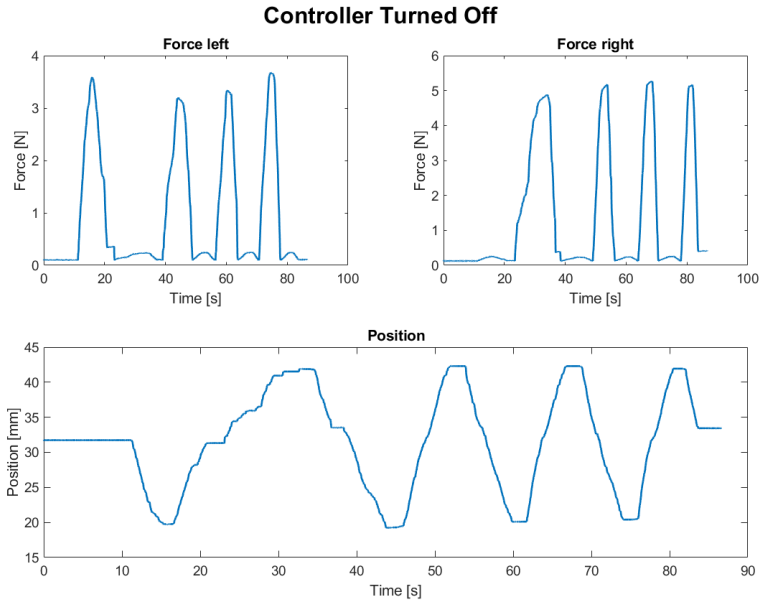

Figure A.8: Force reduction result without any position control and actuation completely turned off.

A.3.2 System Characterisation Example

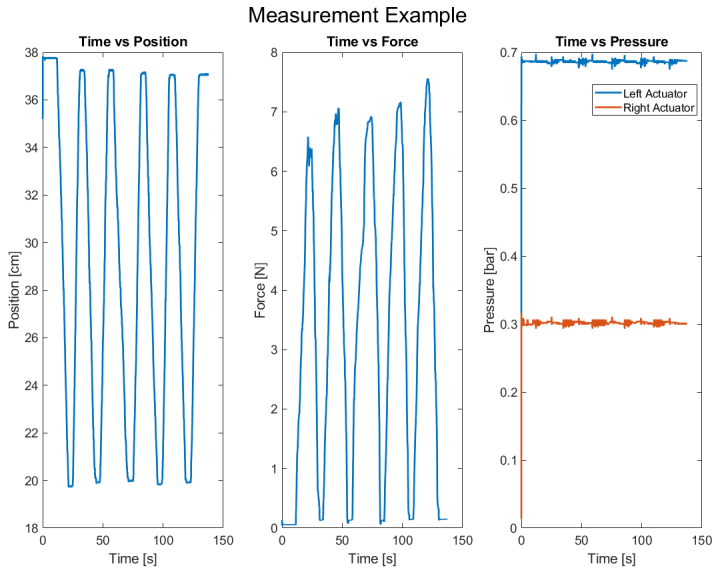

Figure A.9: Results from one of the characterisation measurements. Showing the movement performed, the forces measured on the handle and the pressures in the actuators.

Bibliography

Andrikopoulos, George, George Nikolakopoulos and Stamatis Manesis (Dec. 2014). 'Advanced Nonlinear PID-Based Antagonistic Control for Pneumatic Muscle Actuators'. In: *IEEE Transactions on Industrial Electronics* 61.12, pp. 6926–6937. ISSN: 0278-0046, 1557-9948. DOI: 10.1109/TIE.2014.2316255. URL: https://ieeexplore.ieee.org/document/6786031 (visited on 19/12/2023).

El-Atab, Nazek et al. (Oct. 2020). 'Soft Actuators for Soft Robotic Applications: A Review'. In: *Advanced Intelligent Systems* 2.10, p. 2000128. ISSN: 2640-4567, 2640-4567. DOI: 10.1002/aisy.202000128. URL: https://onlinelibrary.wiley.com/doi/10.1002/aisy.202000128 (visited on 11/02/2024).

Chi, Haozhen et al. (7th June 2021). 'Control of a Rehabilitation Robotic Device Driven by Antagonistic Soft Actuators'. In: *Actuators* 10.6, p. 123. ISSN: 2076-0825. DOI: 10.3390/act10060123. URL: https://www.mdpi.com/2076-0825/10/6/123 (visited on 11/01/2024).

De Jong, Tonke L. et al. (May 2017). 'PVA matches human liver in needle-tissue interaction'. In: *Journal of the Mechanical Behavior of Biomedical Materials* 69, pp. 223–228. ISSN: 17516161. DOI: 10.1016/j.jmbbm.2017.01.014. URL: https://linkinghub.elsevier.com/retrieve/pii/S1751616117300218 (visited on 05/07/2024).

Gudmundsson, Elias S. (30th Oct. 2023). *Evaluation of rPAM actuators for usage in haptic teleoperations*. Publisher: University of Twente. URL: https://essay.utwente.nl/97482/ (visited on 14/07/2024).

Hamed, Abbi et al. (2012). 'Advances in Haptics, Tactile Sensing, and Manipulation for Robot-Assisted Minimally Invasive Surgery, Noninvasive Surgery, and Diagnosis'. In: *Journal of Robotics* 2012, pp. 1–14. ISSN: 1687-9600, 1687-9619. DOI: 10.1155/2012/412816. URL: http://www.hindawi.com/journals/jr/2012/412816/ (visited on 16/04/2024).

Hatzinger, Martin et al. (Nov. 2006). 'Hans Christian Jacobaeus: Inventor of Human Laparoscopy and Thoracoscopy'. In: *Journal of Endourology* 20.11, pp. 848–850. ISSN: 0892-7790, 1557-900X. DOI: 10.1089/end.2006.20.848. URL: http://www.liebertpub.com/doi/10.1089/end.2006.20.848 (visited on 19/06/2024).

Hatzipanayioti, Adamantini et al. (5th Oct. 2021). 'Associations Between Binocular Depth Perception and Performance Gains in Laparoscopic Skill Acquisition'. In: *Frontiers in Human Neuroscience* 15, p. 675700. ISSN: 1662-5161. DOI: 10.3389/fnhum.2021.675700. URL: https://www.frontiersin.org/articles/10.3389/fnhum.2021.675700/full (visited on 17/06/2024).

Klute, G.K., J.M. Czerniecki and B. Hannaford (1999). 'McKibben artificial muscles: pneumatic actuators with biomechanical intelligence'. In: *1999 IEEE/ASME International Conference on Advanced Intelligent Mechatronics (Cat. No.99TH8399)*. 1999 IEEE/ASME International Conference on Advanced Intelligent Mechatronics. Atlanta, GA, USA: IEEE, pp. 221–226. ISBN: 978-0-7803-5038-0. DOI: 10.1109/AIM.1999.803170. URL: http://ieeexplore.ieee.org/document/803170/ (visited on 11/02/2024).

Mack, Michael J. (7th Feb. 2001). 'Minimally Invasive and Robotic Surgery'. In: *JAMA* 285.5, pp. 568–572. ISSN: 0098-7484. DOI: 10.1001/jama.285.5.568. URL: https://doi.org/10.1001/jama.285.5.568 (visited on 01/07/2024).

Maurin, B et al. (1st June 2004). 'A new robotic system for CT-guided percutaneous procedures with haptic feedback'. In: *International Congress Series*. CARS 2004 - Computer Assisted Radiology and Surgery. Proceedings of the 18th International Congress and Exhibition 1268, pp. 515–520. ISSN: 0531-5131. DOI: 10.1016/j.ics.2004.03.326. URL: https:

//www.sciencedirect.com/science/article/pii/S0531513104007599 (visited on 14/07/2024).

Medrano-Cerda, G.A., C.J. Bowler and D.G. Caldwell (1995). 'Adaptive position control of antagonistic pneumatic muscle actuators'. In: *Proceedings 1995 IEEE/RSJ International Conference on Intelligent Robots and Systems. Human Robot Interaction and Cooperative Robots*. 1995 IEEE/RSJ International Conference on Intelligent Robots and Systems. Human Robot Interaction and Cooperative Robots. Vol. 1. Pittsburgh, PA, USA: IEEE Comput. Soc. Press, pp. 378–383. ISBN: 978-0-8186-7108-1. DOI: 10.1109/IROS.1995.525824. URL: http://ieeexplore.ieee.org/document/525824/ (visited on 11/01/2024).

Mendoza, Evelyn and John Peter Whitney (Oct. 2019). 'A Testbed for Haptic and Magnetic Resonance Imaging-Guided Percutaneous Needle Biopsy'. In: *IEEE Robotics and Automation Letters* 4.4. Conference Name: IEEE Robotics and Automation Letters, pp. 3177–3183. ISSN: 2377-3766. DOI: 10.1109/LRA.2019.2925558. URL: https://ieeexplore.ieee.org/document/8747455 (visited on 14/07/2024).

Motheram, Manaswini (16th Oct. 2023). *Force-based measurement of tissue stiffness in 1-DOF needle insertion robotic device for liver interventions*. Publisher: University of Twente. URL: https://essay.utwente.nl/97431/ (visited on 14/07/2024).

Ning, Dayong et al. (1st May 2019). 'Position/force control of master–slave antagonistic joint actuated by water hydraulic artificial muscles'. In: *International Journal of Advanced Robotic Systems* 16.3, p. 172988141985398. ISSN: 1729-8814, 1729-8814. DOI: 10.1177/1729881419853981. URL: http://journals.sagepub.com/doi/10.1177/1729881419853981 (visited on 11/01/2024).

Okamura, A.M., C. Simone and M.D. O'Leary (Oct. 2004). 'Force modeling for needle insertion into soft tissue'. In: *IEEE Transactions on Biomedical Engineering* 51.10. Conference Name: IEEE Transactions on Biomedical Engineering, pp. 1707–1716. ISSN: 1558-2531. DOI: 10.1109/TBME.2004.831542. URL: https://ieeexplore.ieee.org/document/1337139/?arnumber=1337139 (visited on 09/09/2024).

Runciman, Mark, Ara Darzi and George P. Mylonas (Aug. 2019). 'Soft Robotics in Minimally Invasive Surgery'. In: *Soft Robotics* 6.4, pp. 423–443. ISSN: 2169-5172, 2169-5180. DOI: 10.1089/soro.2018.0136. URL: https://www.liebertpub.com/doi/10.1089/soro.2018.0136 (visited on 04/07/2024).

Selim, Mostafa, Douwe Dresscher and Momen Abayazid (Feb. 2024). 'A comprehensive review of haptic feedback in minimally invasive robotic liver surgery: Advancements and challenges'. In: *The International Journal of Medical Robotics and Computer Assisted Surgery* 20.1, e2605. ISSN: 1478-5951, 1478-596X. DOI: 10.1002/rcs.2605. URL: https://onlinelibrary.wiley.com/doi/10.1002/rcs.2605 (visited on 29/01/2024).

Shang, Weijian et al. (2013). 'Teleoperation System with Hybrid Pneumatic-Piezoelectric Actuation for MRI-Guided Needle Insertion with Haptic Feedback'. In: *Proceedings of the ... IEEE/RSJ International Conference on Intelligent Robots and Systems. IEEE/RSJ International Conference on Intelligent Robots and Systems* 2013, pp. 4092–4098. ISSN: 2153-0858. DOI: 10.1109/IROS.2013.6696942.

Shimoga, K.B. (Sept. 1993). 'A survey of perceptual feedback issues in dexterous telemanipulation. I. Finger force feedback'. In: *Proceedings of IEEE Virtual Reality Annual International Symposium*. Proceedings of IEEE Virtual Reality Annual International Symposium, pp. 263–270. DOI: 10.1109/VRAIS.1993.380770. URL: https://ieeexplore.ieee.org/document/380770/?arnumber=380770&tag=1 (visited on 03/10/2024).

Skorina, Erik H., Ming Luo, Wut Yee Oo et al. (12th Oct. 2018). 'Reverse pneumatic artificial muscles (rPAMs): Modeling, integration, and control'. In: *PLOS ONE* 13.10. Ed. by Quanquan Gu, e0204637. ISSN: 1932-6203. DOI: 10.1371/journal.pone.0204637. URL: https://dx.plos.org/10.1371/journal.pone.0204637 (visited on 11/01/2024).

Skorina, Erik H., Ming Luo, Selim Ozel et al. (May 2015). 'Feedforward augmented sliding mode motion control of antagonistic soft pneumatic actuators'. In: *2015 IEEE International Conference on Robotics and Automation (ICRA)*. 2015 IEEE International Conference on Robotics and Automation (ICRA). Seattle, WA, USA: IEEE, pp. 2544–2549. ISBN: 978-1-4799-6923-4. DOI: 10.1109/ICRA.2015.7139540. URL: http://ieeexplore.ieee.org/document/7139540/ (visited on 11/01/2024).

Tavakoli, M., R.V. Patel and M. Moallem (Apr. 2004). 'Design issues in a haptics-based master-slave system for minimally invasive surgery'. In: *IEEE International Conference on Robotics and Automation, 2004. Proceedings. ICRA '04. 2004.* IEEE International Conference on Robotics and Automation, 2004. Proceedings. ICRA '04. 2004. Vol. 1. ISSN: 1050-4729, 371–376 Vol.1. DOI: 10.1109/ROBOT.2004.1307178. URL: https://ieeexplore.ieee.org/document/1307178/?arnumber=1307178 (visited on 03/10/2024).

Tse, Zion Tsz Ho et al. (Feb. 2012). 'Haptic Needle Unit for MR-Guided Biopsy and Its Control'. In: *IEEE/ASME Transactions on Mechatronics* 17.1. Conference Name: IEEE/ASME Transactions on Mechatronics, pp. 183–187. ISSN: 1941-014X. DOI: 10.1109/TMECH.2011.2113187. URL: https://ieeexplore.ieee.org/document/5727956 (visited on 14/07/2024).

Vicentini, M. et al. (Oct. 2010). 'Evaluation of force and torque magnitude discrimination thresholds on the human hand-arm system'. In: *ACM Trans. Appl. Percept.* 8.1, pp. 1–16. ISSN: 1544-3558. DOI: 10.1145/1857893.1857894. URL: https://doi.org/10.1145/1857893.1857894.

Wagner, C.R., N. Stylopoulos and R.D. Howe (2002). 'The role of force feedback in surgery: analysis of blunt dissection'. In: *Proceedings 10th Symposium on Haptic Interfaces for Virtual Environment and Teleoperator Systems. HAPTICS 2002.* 10th Symposium on Haptic Interfaces for Virtual Environment and Teleoperator Systems. HAPTICS 2002. Orlando, FL, USA: IEEE Comput. Soc, pp. 68–74. ISBN: 978-0-7695-1489-5. DOI: 10.1109/HAPTIC.2002.998943. URL: http://ieeexplore.ieee.org/document/998943/ (visited on 18/06/2024).